Distribution Agreement

In presenting this thesis or dissertation as a partial fulfillment of the requirements for an advanced degree from Emory University, I hereby grant to Emory University and its agents the non-exclusive license to archive, make accessible, and display my thesis or dissertation in whole or in part in all forms of media, now or hereafter known, including display on the world wide web. I understand that I may select some access restrictions as part of the online submission of this thesis or dissertation. I retain all ownership rights to the copyright of the thesis or dissertation. I also retain the right to use in future works (such as articles or books) all or part of this thesis or dissertation.

Signature:

_____ _____

Dylan James Collette Date

Effects of macromolecular crowding on DNA structure and protein-mediated DNA looping. hKIF4a compaction of DNA

By

Dylan James Collette
Doctor of Philosophy

Physics

Laura Finzi, Ph.D
Advisor

David Dunlap, Ph.D
Advisor

Justin Burton, Ph.D.
Committee Member

Kurt Warncke, Ph.D.
Committee Member

Keith Weninger, Ph.D
Committee Member

Accepted:

Kimberly J Arriola, Ph.D., MPH
Dean of the James T. Laney School of Graduate Studies

Date

Effects of macromolecular crowding on DNA structure and protein-mediated DNA looping. hKIF4a compaction of DNA

By

Dylan James Collette
B.S., West Chester University of Pennsylvania 2017

Advisors: Laura Finzi, Ph.D and David Dunlap, Ph.D

An abstract of
A dissertation submitted to the Faculty of the
James T. Laney School of Graduate Studies of Emory University
in partial fulfillment of the requirements for the degree of
Doctor of Philosophy
in Physics
2022

Abstract

Effects of macromolecular crowding on DNA structure and protein-mediated DNA looping. hKIF4a compaction of DNA
By Dylan James Collette

The cellular environment is highly crowded, but many laboratory measurements are conducted in dilute buffer. In order to begin to bridge the gap between *in vitro* and *in vivo* measurements, macromolecular crowders are often included in *in vitro* experiments. An extensive survey of the literature indicated that experiments with biologically relevant crowders, experiments with mixtures of variously sized crowders, and experiments elucidating information on the interplay between macromolecular crowding and liquid-liquid phase separation within the cell all require further work. Tethered particle motion experiments were designed to directly investigate the effects of macromolecular crowding on protein-mediated looping in DNA. Macromolecular crowding caused DNA to preferentially adopt the parallel loop conformation over the anti-parallel loop conformation. Another set of tethered particle motion experiments were performed to characterize the compaction of DNA by the protein hKIF4a, a chromokinesin. hKIF4a required ATP to compact DNA, although a truncated form of hKIF4a lacking the ATPase domain, compacted DNA better than wild-type hKIF4a in the presence of AMP-PNP, an non-hydrolyzable ATP analogue.

Effects of macromolecular crowding on DNA structure and protein-mediated DNA looping. hKIF4a compaction of DNA

By

Dylan James Collette
B.S., West Chester University of Pennsylvania 2017

Advisors: Laura Finzi, Ph.D and David Dunlap, Ph.D

A dissertation submitted to the Faculty of the
James T. Laney School of Graduate Studies of Emory University
in partial fulfillment of the requirements for the degree of
Doctor of Philosophy
in Physics
2022

Acknowledgments

I have deep gratitude for my advisors, Dr. Laura Finzi and Dr. David Dunlap for their guidance and support over the last few years that I have been in their lab.

I am also immensely grateful for my committee members: Dr. Justin Burton, Dr. Kurt Warncke, and Dr. Keith Weninger for the discussions provided, time given, and attendance to my annual meetings.

I would like to specifically recognize Barbara Conner for her constant support and assistance throughout my 5 years at Emory, I never would have made it this far without her.

I would like to also thank my colleagues, Wenxuan Xu assisting me throughout my studies; Jin Qian for assisting with the data analysis of my data.

I owe my parents, Kevin Collette and Gretchen Collette for their constant support and motivation over the last 5 years of my studies, as well as my siblings, Molly Collette and Heather Leva.

I would also like to acknowledge my personal hero, Stephen Robert Irwin, for inspiring my curiosity and passion for nature.

I also have to give a shoutout to the staff and patrons of 529 and Flatiron, I love you all!

Finally, I would like to thank my wonderful wife, Krysta Collette, to whom this dissertation is dedicated.

Contents

List of Figures

Chapter 1

Introduction

In this dissertation I will discuss my research on the effects of macromolecular crowding on DNA structure and protein-mediated DNA looping. I will also be discussing my tethered particle motion experiments investigating hKIF4a compaction of DNA. This dissertation will begin with a broad review on the effects of macromolecular crowding on DNA structure, where I will identify gaps in the research that I provide motivation to investigate. While the cellular environment is highly crowded, most laboratory measurements are conducted in dilute buffers; adding macromolecular crowders to experiments is one way to begin bridging the gap between *in vitro* and *in vivo* measurements. The review begins with previous works investigating the effects of macromolecular crowding on the compaction and extension of DNA, from which it can be seen that synthetic polymers such as polyethylene glycol (PEG) or dextran as crowders, as opposed to physiologically relevant crowders such as RNA or proteins are commonly used. The next section of the review discusses the effects of macromolecular crowders on the kinetics of DNA; with one of the main focuses being the effects of the size of crowders. Many groups, described within this dissertation observed that only large crowders effect the kinetics of DNA in ways other than increasing the viscosity of the buffer [2, 3, 4]. In most investigations into the effects

of macromolecular crowder size, only one size crowder is used at a time, while the cellular environment contains crowders of varying sizes, motivating further research with macromolecular crowders of varying sizes simultaneously. This section also discusses the connection between liquid-liquid phase separation (LLPS) and the crowded cellular environment; experiments connecting LLPS, macromolecular crowding, and nucleic materials have not yet been reported. This chapter wraps up with a discussion of theoretical works modeling polymer chains in a crowded solution.

The next chapter discusses my experimental work on the effects of macromolecular crowding on protein-mediated looping of DNA. These experiments were conducted using the tethered particle motion (TMP) measurements, which is a simple, yet powerful single-molecule measurement technique. In TPM, a strand of DNA is anchored to a substrate on one end (a glass coverslip in this case) and attached to a bead on the other end. The bead traverses a hemisphere, the radius of which is limited to the length of the DNA tether. The 2D projection of the bead is tracked and recorded to elucidate information about the length of the tether. During protein-mediated looping (LacI-mediated looping) the DNA may sample two different loop conformations, parallel and anti-parallel loops. Anti-parallel loops require more DNA than the parallel loops, which shortens the effective tether length to a further extent. The macromolecular crowders investigated in this section were dextran 70 (70 kDa) and bovine serum albumin (BSA, 66.5 kDA). These measurements indicate that in the presence of macromolecular crowders, DNA favors the parallel loop conformation over the anti-parallel loop conformation. One possible explanation for this is that macromolecular crowders decreased the compatibility with the solvent, causing the DNA to favor self-interactions over interactions with the solvent.

The fourth chapter of this dissertation discusses further TPM experiments I conducted to characterize hKIF4a compaction of DNA. KIF4a is a chromokinesin that has been hypothesized to contribute to the organization of mitotic chromosomes and

the formation of chromosomal scaffolding. Measurements began with bare DNA, in the absence of hKIF4a as a buffer, and then continued with a truncated version of the protein that had the DNA binding domain removed; results with the truncated variant of the protein were indistinguishable from those with the bare DNA. Measurements were then conducted with both 10 and 50 nM hKIF4a in the presence of both ATP and AMP-PNP (a non-hydrolysable analogue of ATP). These measurements showed significantly higher rates of compaction in the presence of ATP when compared to AMP-PNP, leading to the conclusion that hKIF4a utilizes ATP to compact DNA. I next increased the concentration of hKIF4a to 100 nM in the presence of ATP and found that every tether compacted. At 250 nM hKIF4a, every tether observed appeared to maximally compact on the surface of the substrate. The next set of measurements involved a mutant of hKIF4a with the ATPase deleted; DNA incubated with the mutant hKIF4a without ATPase more compacted than the wild-type hKIF4a in the presence of AMP-PNP, but less than the DNA incubated with wild-type protein in the presence of ATP. A final set of experiments with hKIF4a investigated the effects of macromolecular crowding on hKIF4a-induced compaction of DNA. A set of control experiments was conducted, in the presence of 5% BSA (w/v) without hKIF4a and no compaction was observed, whereas in the presence of hKIF4a and 5% BSA there was significant compaction of the DNA.

Chapter 2

Effects of macromolecular crowding on DNA structure

2.1 Introduction

Biological sciences have long sought to mimic *in vivo* conditions *in vitro*. Due to the complexity of living cells, there are many obstacles to emulating cellular environments within the laboratory setting. Biological cells are highly crowded by macromolecules of varying sizes, structures, and charges including cytoskeletal protein filaments, dissolved salts, proteins, and nucleic acids [5]. This complex, crowded environment plays a key role in a variety of biological processes and functions including viral infection, gene expression, chromosomal compaction, replication, and transcription [6, 7, 8, 9, 10]. The full extent of the impact that crowding has on the dynamics of nucleic acids in the cell remains a vigorous avenue of research. On average, the volume fraction of a cell that is taken up by solute molecules is 30%, although this value can rise up to 40% [11, 10, 7, 8, 12]. It is currently accepted that all cells are highly compartmentalized even in the absence of membrane-enclosed organelles, which locally concentrates specific groups of molecules and enhances crowding effects

[13]. Additionally, the cytoplasm and its contents are highly limited by the cellular membrane to dimensions a few micrometers in diameter for bacteria, and tens of micrometers for eukaryotic cells [7]. Crowding created by membrane confinement has proven difficult to reproduce and is often neglected in *in vitro* experiments. Although a variety of small molecules contribute to crowding, in this review we will focus on the effect of polymers. The manner in which crowding, by macromolecules (macromolecular crowding) affects nucleic acids and their transactions is highly relevant to understanding genome structure and function and relating *in vitro* to *in vivo* observations [9, 14, 15, 16].

2.2 Compaction and extension of DNA

An *Escherichia coli* (*E. coli*) cell is around one micron in length, while the length of the DNA contained within is over a millimeter [17]. The cellular environment is also very crowded, with volume fractions of 30-40% being occupied by various organelles and nucleic materials [10, 7, 18, 11, 8, 12]. The relationship between molecular crowding and DNA compaction is one of great interest to understand the forces driving DNA packaging and architecture. Compaction or condensation of DNA is usually defined as the collapse of extended DNA chains into more dense structures such as rods, fibers, flexible rings, toroids, and hierarchical coils [19]. The compaction of DNA plays a key role in genome organization within the cell and is a fundamental constraint on the efficient storage and processing of genetic information. In prokaryotes, this major function is accomplished via the interplay of three crucial factors, DNA supercoiling [20], macromolecular crowding and nucleoid-associated proteins (NAPs) [21, 22, 23, 24, 25, 26]. In general, the compaction of DNA chains may be induced by a variety of agents such as multivalent macro-cations [27, 28, 29], cationic lipids [30], detergents [31], peptides [32], and many polymers [33, 34], and is highly relevant

in biology and gene therapy, calling for thorough studies. DNA extension, or decondensation, is crucial, on the other hand, to allow access to the double helix. Tuning condensation/decondensation of DNA is clearly fundamental for regulation of cellular activities.

2.2.1 Polyethylene glycol

Polyethylene glycol (PEG) is a neutral polymer that is utilized in industrial manufacturing and medicine. PEG is a polyether compound derived from petroleum, and has been widely used in medicine due to its biocompatibility, low or non-toxicity features, and high solubility [35, 36]. For example, PEG has been used to carry therapeutic DNA for gene delivery [37]. In the presence of salts, PEG can induce DNA condensation through a process commonly referred to as polymer and salt-induced (psi, Ψ) condensation [38, 39], which was first described by Lerman in 1971 [34]. There have since been many experimental studies investigating the phenomenon of Ψ condensation [40, 41, 42, 43, 44, 45, 46, 47, 48, 49, 50, 51]. Vasilevskaya *et al.* investigated the compaction of a single DNA molecule in a PEG solution via fluorescence microscopy [48]. They found that the critical concentration of PEG required to induce DNA compaction decreases with increasing degree of PEG polymerization and salt concentration. The physical explanation of DNA collapse in PEG solutions given by Vasilevskaya [48] is that the contacts between DNA and PEG are thermodynamically unfavorable. Thus, the solvent quality for DNA becomes poorer upon the addition of PEG, meaning that the effective attraction between the segments of DNA macromolecule increases.

Ramos *et al.* found the critical concentration of PEG required to induce DNA condensation as a function of NaCl concentration using DNA fragments of about 4 kbp and PEG with degrees of polymerization ranging from 45 to 182 via circular dichroism (CD) spectroscopy [47]. They found that there was a significant depen-

dence on the degree of polymerization of PEG in agreement with Vasilevskaya. They also reported phase separation boundaries for the intermolecular condensation that were very similar to those observed previously for intramolecular collapse [38, 52]. Intermolecular DNA condensation has many similarities with intramolecular DNA condensation, and both forms of collapsed DNA can be resolubilized by further addition of neutral polymer [48]. Additionally, very dilute solutions of long DNA, for both inter- and intramolecular collapse had a strong dependence on the concentrations of PEG and salt [48, 49]. Using a 40 mM DNA solution in 0.2 M NaCl to which different amounts of (w/w) of PEG 2000 were added, Ramos *et al.* [47] found that changing the PEG concentration from 19% to 20% yielded a 10 times more intense spectrum, with a broad negative band displaced from 240 nm to 270 nm, and a positive band displaced from 275 nm to above 300 nm as is characteristic for Ψ condensation [53]. Continuing addition of PEG to 22% leads to the reduction of the negative band intensity, and return to the spectrum typical of the B conformation, indicating a process that they refer to as 'reentrant decondensation'. Ramos states that for DNA decondensation, the flexible polymer (PEG in this study) concentration needs to be increased to a point where DNA leaves the Ψ configuration and is most probably a disperse solution. The same authors reported that for most decondensation experiments the concentration of PEG was increased until decondensation was observed. Experiments in which the salt concentration was increased at a fixed concentration of PEG yielded the same results, suggesting that thermodynamic equilibrium had been attained.

Cheng *et al.* studied the DNA condensation induced by PEG of varying molecular weights in the presence of monovalent salt (NaCl) as well as divalent salt ($MgCl_2$) [54]. Through magnetic tweezer (MT) experiments they found that with increasing NaCl concentrations, the critical condensation force in the PEG-DNA solution increased approximately linearly, with the higher molecular weight PEG solution

having a larger critical force than the lower molecular weight PEG solution. The divalent salt system, in comparison, followed a parabolic trend of the critical condensation force as a function of increasing $MgCl_2$ concentration. They first examined the effects of experimental buffer conditions (100 mM Tris-HCl) on the DNA condensation and found that without the addition of salts there was no detectable transition found in the PEG 600 solution (30% w/v), where 600 indicates the molecular weight in Da. It was found that at least 300 mM Na^+ was required in order to observe this transition. Alternatively, the PEG 6000 solution alone was able to induce DNA condensation in the absence of salts. By varying PEG 6000 concentration, it was found that the critical force produced during condensation decreased from the ∼0.6 pN at 30% PEG concentration to ∼0.1 pN at 18% PEG concentration. There was no detectable condensation transition in PEG 6000 solutions with concentrations under 18%. Cheng *et al.* concluded that the added salts (Na^+ or Mg^2+) play an important role in the Ψ condensation. Cheng also observed samples via atomic force microscopy (AFM) and found that the morphologies of the compacted DNA-PEG complexes had a dependence on the salt concentration and were consistent with the MT results.

Scott *et al.* conducted single molecule Convex Lens-induced Confinement (CLiC) experiments and found that crowding agents affect DNA binding and unwinding [7]. They state that molecular crowders are assumed to influence binding events mostly through collisions with other molecules and that assessing whether crowders exert specific effects on binding at physiological ionic strength is of interest. Using 8 kDa PEG (PEG 8000), 10 kDa polyvinylpyrrolidone (PVP), and 55 kDa PVP at 12.5% w/v with an ionic concentration of 150 mM (137.4 mM NaCl, 12 mM Tris, 25 mM HEPES, pH 8.0) and a temperature of 37°C, they investigated this phenomena. Under these conditions, only NaCl ions dissociate completely yielding an ionic contribution of 12.5 mM from both Tris and HEPES. All experiments with crowding agents showed an increase in DNA-DNA binding as opposed to control measurements with no crowding

agent. Since there was no significant difference observed from different specific species or sizes of crowding agents, following experiments were conducted with 8 kDa PEG as the crowding agent. Further measurements used similar experimental conditions as before, but investigating the effects of increasing concentrations of 8 kDa PEG over a range of 0%, 1%, 5%, 10%, and 20% (w/v). An increase in binding with increasing PEG concentration was observed. Additionally, the dependence of salt concentration was investigated over a range of 10 mM to 137.5 mM of NaCl to observe the effects of monovalent ionic concentration on plasmid-probe binding. Factoring in the ionic contributions of NaCl found within the 12 mM Tris and 25 mM HEPES brings the total ionic concentration into the range of 22.5-150 mM. Physiological ionic conditions are considered to be concentrations between 100 and 200 mM [55]. Scott *et al.* [7] found that as salt concentrations increased, DNA-DNA binding decreased; this is expected to be due to the increase in positively charged ions screening the negative charges on the DNA. Therefore, in low ionic strength conditions the repulsion between the negatively charged phosphate backbone produces denaturation of segments of plasmid DNA that allows DNA-probe interactions [56, 57]. Rybenkov, *et al.* also found that increased ionic strength decreased the free energy of supercoiling of DNA [56], which in turn reduces the probability of unwinding, resulting in a decrease of probe binding. In order to determine whether a decrease in unwinding, a reduction in the reaction rate between the plasmid and probe, or some cooperative effects between the two accounted for the reduction in binding, Scott *et al.* plotted the initial amount of unwound plasmid and the rate of binding versus ionic strength. A second-order reaction model was used to estimate binding rates and determine the unwound state of plasmids, this model assumed the rates of unwinding and rewinding are negligible compared to the rate of binding, consistent with previous results from Scott *et al.*

[58]. This second-order reaction equation can be expressed as

$$[B] = [U]_0(1 - e^{-k't})$$

where k' is a constant, t is time, $[U]_0$ is the initial concentration of unwound plasmids, and B is the concentration of bound complexes. The constant K is used to determine the rate of reaction through the expression $K = k([P]_0 - [U]_0)$, where k is the true rate constant for this reaction, and $[P]_0$ is the initial concentration of probe molecules [58]. Using the fits to this equation, the initial amount of unwound plasmid decreases with increasing ionic strength, while the rate of binding to unwound sites does not vary significantly for all ionic strengths observed in this study. Once it was observed that the rate of binding to unwound sites did not vary significantly for the observed salt concentrations in the absence of crowding agents, macromolecular crowders were once again added to the sample, and were found to have strong effects. It was found that binding increased with ionic concentration in the presence of crowding agents. Using similar experimental conditions as previously reported, but with the addition of 10% (w/v) 8 kDa PEG and increasing NaCl concentrations they observed that binding between the probe and plasmid increased with increasing ionic strength in the presence of crowding agents, as opposed to the absence of crowding agents.

Mardoum *et al.* reported that crowding induces entropically-driven changes to DNA dynamics, they stated that these changes depend on crowder structure and ionic conditions [6]. Upon examining the role of crowder structure on DNA conformation and diffusion, they found that branched, compact crowders such as PEG and Ficoll drive DNA to compact, while linear, flexible crowders such as dextran caused DNA to elongate. They observed that the extent to which DNA mobility is reduced by increasing crowder concentration appears largely insensitive to crowder structure, despite crowder structure causing the DNA to take on highly different configurations.

Cristofalo *et al.* conducted magnetic tweezer (MT) experiments to investigate the effects of PEG on the compaction of DNA fragments in cooperation with the nucleiod protein H-NS [21]. The structural role of H-NS and/or PEG on DNA was investigated in assays, where the DNA collapse/loop-formation mechanism was monitored using the extension of the DNA in response to the externally applied force on a magnetic bead that was attached to the end of the DNA molecule. PEG force-extension curves were consistent with teasing the DNA filament out of a collapsed globule. In the absence of PEG alone, at a 16% volume fraction, DNA condensation was induced, with respect to the behavior of bare DNA. In the presence of PEG the force-extension curves show a transition between a very stiff regime detected at low force, where a characteristic force value ($\sim$ 0.6 pN) is required to observe any extension. Above this critical force, the DNA polymer was reported to extend with no energy cost, where the DNA extension increased from zero to a maximum extension value for bare DNA with no increase to the applied force. They stated that above this critical force, the force-extension curve appears to be compatible with the one measured for DNA in the absence of PEG, which was interpreted as the behavior associated with teasing a DNA filament out of equilibrium within a collapsed globule, which has been well-studied [59, 60, 61]. Cristofalo *et al.* divided this observed behavior into three distinct regimes; in the first (low-force) regime, the extension is associated with elastic deformation of an intact globule (prolate configuration). In the second (free pulling) regime, a linear chain of monomers is extended from the globule as a 'tail' forming several different 'tadpole' configurations whose energy costs are balanced by the gain in entropy for the free part of the chain (tail). The third regime represents the fully extended polymer.

Previous works have shown that branched crowders, such as PEG and ficoll (not discussed here), tend to induce compaction in DNA, while linear crowders, like dextran (see below) initialy cause DNA to elongate, but as crowder concentration is

increased, will also induce compaction of DNA.

2.2.2 Dextran

Dextran is another polymer that is commonly used in macromolecular crowding experiments, it is a complex branched glucan (polysaccharide derived from the condensation of glucose), originally derived from wine. The Union of Pure and Applied Chemistry (IUPAC) defines dextrans as "Branched poly-α-d-glucosides of microbial origin having glycosidic bonds" [62]. Dextran has been used *in vitro* to mimic the intracellular crowding of DNA to understand the compaction of linear and plasmid DNA [63, 64, 65, 66]. Plasmid DNA exhibits different compaction from linear DNA under crowding [63]. Crowding affects characteristics of DNA superhelicity such as the degree of interwinding and the number of interwound branches of plasmids [63, 67].

Mardoum *et al.* used single molecule fluorescence microscopy and particle tracking algorithms to investigate the effects of macromolecular crowders on the transport and conformational dynamics of large DNA molecules [6]. They measured the mean-squared center of mass displacements as well as the conformatioonal size, shape, and fluctuations of individual 115 kbp strands of DNA that were diffusing through various *in vitro* solutions of macromolecular crowders. The role of crowder structure and concentration was determined, along with ionic conditions, on the diffusion and configurational dynamics of DNA. Linear, flexible polymers, such as dextran, were found to cause DNA to elongate. The diffusion and conformational dynamics of DNA crowded by dextran of varying molecular weights and concentrations had been previously measured and it was found that the decrease in DNA diffusivity with increasing dextran concentrations was less than expected based on the increasing viscosity of the crowding solutions [68, 69]. It was found that the measured diffusion coefficients followed a weaker scaling with viscosity than the expected classical Stokes-Einstein scaling $D \sim \eta^{-1}$.

Gupta and Maarel conducted laser light scattering measurements to measure the radius of gyration of pHSG298 plasmids with a length of 2675 bp in supercoiled and linear configurations in the presence of macromolecular crowding [64]. They observed that the supercoiled form initially expands and subsequently compacts as the volume fraction of the crowder increases. The extent of this expansion was found to be highly dependant on the size of the nanoparticle crowders, with the smallest particles exhibiting the largest effect. The linear plasmid experienced monotonous compaction with increasing crowder volume fraction and there was no peak in the radius of gyration observed.

Khatun *et al.* performed static/dynamic light scattering (S/DLS) experiments with different plasmid-dextran combinations in order to elucidate information on the effect of crowder size on plasmid compaction [63]. They used three plasmids (pBS, 2.9 kbps; pCMV-Tag2B, 4.3 kbps; and pET28a, 5.3 kbps) that were isolated and purified in supercoiled configurations. The results from this study indicated the presence of two compaction regimes for plasmid-dextran combinations that were quantified in terms of the radius of gyration, R_g. The diffusivity of plasmids in these two regimes was observed to be dictated by normal diffusion in one regime, and subdiffusion (the tendency of particles in a fluid to diffuse anomalously slowly due to trapping) in the other. Khatun interpreted the regimes as the outcome of an imbalance between the the osmotic pressure caused by the entropically driven depletion forces from dextran and the elastic pressure resulting from conformational changes in the plasmid under crowding. They state that within these two regimes of compactions experienced by plasmids, the plasmid conformation is sensitive to the size of crowders, and the compaction is quantified in terms of R_g which is estimated for different plasmid-dextran combinations via laser light scattering. Khatun *et al.* proposed a generalized scaling law of R_g as

$$R_g \cong \xi(x) R_{g0}^{2/(1+x)} d^{2/(1+x)} \psi^{-1/(1+x)}$$

where R_{g0} is the radius of gyration of plasmids in the uncrowded environment, $\xi(x)$ is the prefactor representing the deviation of plasmid conformation from its conformation in the absence of crowding, ψ is the volume fraction of the crowding agent, and x is the measure of the conformational geometry of the plasmids. This equation was derived by equating the elastic pressure due to plasmid conformational changes to the osmotic pressure that arise from depletion forces due to the crowders.

Previous work has shown that the molecular weight of dextran is a key parameter when conducting measurements. Relatively low molecular weights of dextran cause DNA to extend, but as molecular weight and volume fraction is increased, DNA will subsequently compact.

2.2.3 Bovine serum albumin

Bovine serum albumin (BSA) is a protein derived from cows and is often used as protein supplement in cell culture media [70]. BSA is a small, stable, and moderately non-reactive protein [71] with isoelectric point at pH=5.1-5.5, and a molecular weight of 66.5 kDa.

Liu *et al.* conducted Förster resonance energy transfer (FRET) measurements using crowding-sensitive probes (pairs of flourophores linked in close proximity) and found that BSA induced compression of the probes [72]. They found that the degree of compression was directly related to the concentration of BSA throughout their measurements. The probes were found to compress with a magnitude that depended on the probe and the crowder; compression scaled with probe size, and for fixed crowder weight %, depended on crowder hydrodynamic radius.

The vast majority of publications investigating macromolecular crowding using

biologically relevant crowders tend to focus on the effects on other proteins and not specifically what impact they have on DNA. It is clear that more work needs to be done to investigate what effects biologically relevant macromolecular crowders have on DNA.

2.2.4 Outlook

The effects of macromolecular crowding on the compaction and extension of DNA have been heavily investigated. The overwhelming majority of research has focused on the effects of non-physiological, neutral crowders such as polyethylene glycol and dextran. These crowders are so widely used because they are non-interacting, for the most part, and commercially available. Going forward, to further bridge the gap between *in vitro* and *in vivo* experiments, a systematic analysis of the effect of size, shape, and charge of crowder should be conducted on various aspects of DNA properties and functions, including DNA-protein interactions, DNA topology, DNA repair, recombination, etc. In addition, wider range of biologically-relevant macromolecular crowders should be explored, including nucleic acids and cytoskeletal filaments normally present in the nucleus/nucleoid.

2.3 Kinetics

2.3.1 Crowders vs. viscogens

Chung *et al.* investigated the effects of macromolecular crowding on transcription initiation by *E. coli* RNA polymerase (RNAP) [2]. With up to 40% of the overall volume of the cytoplasm taken up by macromolecules [8, 11, 7, 10, 18, 12], *E. coli* cells present a dense environment that is likely to affect biological reactions, as compared to the same reactions in buffer [73, 74, 75, 76], due to the drastic increase in viscosity that slow macromolecular motions and kinetics [77, 78].The volume ex-

clusion due to this level of crowding affects the thermodynamics and/or kinetics of reacting molecules. Transcription is often investigated *in vitro* [79, 80, 81] yielding results that sometimes differ from *in vivo* observations, in part due to environmental factors such as the macromolecular crowding [82, 83]. Chung *et al.* found that only large crowders affect transcription kinetics in other ways than viscosity. Measurements were conducted using *in vitro* quenching-based single-molecules kinetics assays. Microviscosity measurements were conducted using fluorescence correlation spectroscopy (FCS). The microviscosity for RNAP-Promoter complexes were measured under various crowder conditions, and all measurements were performed at 25°C using a confocal microscope with a continuous wavelength laser at 532 nm. The transcription initiation quenched-kinetics assay quantified the number of transcripts at each time point, defined by the time a reaction quencher was added [84]. Once the transcription reaction is stopped by the quencher, the added ssDNA FRET probes hybridize to the transcribed RNAs during an incubation period. Transcription initiation was tested with 25% Glycerol, 15% PEG8000, 15% Ficoll70, and 5% Dextran500 (w/v). Transcription initiation rates in buffer were also measured as a reference for behavior in the absence of viscogens or macromolecular crowders. Measurements revealed that rates of elongation in polymer solutions such as PEG, Dextran, or Ficoll, are faster than the kinetics in 25% glycerol, even though the viscosities of the polymer solutions are much higher than that of 25% glycerol. Since the effective viscosity in a crowded medium (the microviscosity) could differ from the bulk viscosity of the medium [85, 86, 87], FCS experiments were performed to estimate the actual viscosities experienced under various crowding environments. FCS measurements showed that microviscosities for the large crowders, Ficoll70 and Dextran500 are much smaller than their macroviscosities, while Dextran10 and PEG8000 had microvascosities comparable to their macroviscosities. A unidirectional first-order kinetics model was used to fit and extract kinetic rate constants in order to better understand the effects of

various sized crowders on transcription kinetics. The extracted rates were adjusted using Kramers kinetic theory to account for viscosity effects and decouple them from the crowder volume exclusion effects [88]. It has been demonstrated several times that the effect of viscosity on some protein folding kinetics follow Kramers theory [89, 90, 91]. The viscosity-adjusted kinetics rate constants showed acceleration by a factor of ~ 2 for dextran500 and ficoll70, and ~ 6 for PEG8000, while the viscosity-adjusted rate constants for glycerol was only marginally affected. This is due to the fact that glycerol is a viscogen and does not act as a macromolecular crowder. Chung *et al.* concluded that only large crowders affect the transcription kinetics in other ways than viscosity and therefore act as macromolecular crowders [2].

Stiehl *et al.* found that macromolecular crowding slows down the stochastic opening and closing of single-strand DNA (ssDNA) hairpins, but also increases the steady-state fraction of closed hairpins significantly [3]. This increase in the fraction of closed hairpins was shown to increase if the crowding was associated with subdiffusion. It was concluded that biochemical reactions in crowded fluids are sensitive to both volume exclusion effects and changes of the reactants' diffusion characteristics. To observe the conformational fluctuations of a ssDNA hairpin, Stiehl *et al.* followed the approach of Bonnet *et al.* [92] and Wallace *et al.* [93, 94]. The kinetics of the ssDNA constructs (beacons and controls) were monitored in water containing varying amounts of sucrose. Increased concentrations of sucrose increses the viscosity of the fluid, but does not lead to subdiffusion of tracer particles [95]. The sucrose solution acts as a purely viscous medium, where the hairpin opening and closing rates are expected to change similarly with increasing viscosity, and therefore the sucrose concentration. The beacon's closing rate was approximated as a diffusive search of two binding partners separated by the ssDNA length, while the opening rate was described by Kramer's escape rate from a local potential minimum. Following this analysis, the mean residence time in the hairpin conformation was expected to grow

with increasing sucrose concentration with the steady-state fraction of open hairpins remaining independent of sucrose concentration. However, there was significantly lower fraction of open hairpins as the concentration of crowding agents increased, in addition to the slowing down of the conformational fluctuations that were also observed for viscogens. The observed changes of the steady-state fraction of closed ssDNA hairpins were significant for 10 kDA-, 4kDA- PEG and dextran, while 200 Da-PEG (which is comparable in size to sucrose molecules) had no significant effect on the steady-state fraction of closed hairpins. UV absorption measurements confirmed the observed change in the fraction of closed hairpins in crowded fluids, measured via FCS; the fraction was closed hairpins was reduced by about 16% by PEG and 70% by dextran, as compared to the sucrose solution. It was also observed that changes in temperature from 25 to 60°C only lead to minor changes in the absorption levels. The observed crowding-induced closing of the ssDNA hairpin was strongest when using high concentrations of crowders. While both PEG and dextran exhibited similar effects on closing hairpins, there is a stark difference between the structure of the two: 10 kDa-PEG is a linear polymer with a hydrodynamic radius of ∼2.8 nm [96], while dextran of the same weight is a branched polymer with a hydrodynamic radius of ∼1.8 nm [97]. Stiehl *et al.* determined that the apparent volume occupancy of 10 kDa-PEG is about 3.8 fold larger than that of dextran [3].

In summary, previous work has shown that the size of crowders is a key factor. Larger molecular weights yield crowding effects such as caging or trapping due to entropic effects from volume exclusion, while smaller molecular weights of crowders will intermix with the DNA and only increase the viscosity of the solution.

2.3.2 Phase separation

As far back as 1995, Walter and Brooks hypothesized that phase separation in the cytoplasm, due to macromolecular crowding, is a basis for microcompartmentaliza-

tion [98]. Levone *et al.* determined that FUS-dependent liquid-liquid phase separation (LLPS) is important for DNA repair initiation [99]. Their experiments did not involve macromolecular crowding, but definitively showed that LLPS has important cellular functions. Shakya *et al.* investigated LLPS of histone proteins in cells to determine its role in chromatin organization [100]. Histone proteins package cellular DNA into actively transcribed euchromatin domains as well as suppressed heterochromatin domains. Through *in vivo* (in cell) and *in vitro* studies, it was found that histones contribute to heterochromatin formation through reversible LLPS with DNA. In this case, the LLPS forms liquid droplets containing linker histome H1 and chromatin, and they likely govern the access of transcription factors and RNA to heterochromatin domains through charge balance, multicomponent interactions, and fluctuating levels of small molecules such as ATP.

Park *et al.* conducted experiments and field-theoretic simulations via complex Langevin sampling that suggest PEG drives LLPS by dehydration of polymers [101]. The investigation focused on the coacervate phase, an aqueous phase rich in macromolecules such as synthetic polymers, proteins, or nucleic acids [102, 103, 104, 105, 106]. Complex coacervation (CC) is a phenomenon in which polyelectrolytes separate into a polyelectrolyte-dense phase and a polyelectrolyte-dilute phase [107]. CC is affected by a wide variety of influences, such as ionic strength, pH, polyelectrolyte concentration, molecular weight of the polyelectrolytes, as well as temperature, and crowding pressure [108]. Experimental measurements were taken through fluorescence recovery after photobleaching (FRAP), within the coacervate phase, in the absence and presence of PEG.

Kohata and Miyoshi published a short review in 2020 titled *RNA phase separation-mediated direction of molecular trafficking under conditions of molecular crowding* [5]. Selective interactions and specific functions of biomolecules are controlled in a temporal- and spatial-specific manner in complex crowded environments involving

numerous other biomolecules. The collective and congregative effect of biomolecular properties and behaviors that facilitate specific interactions between biomolecules has attracted considerable research attention in recent years [109, 110]. Biomolecular localization systems using droplets formed via LLPS as observed in the cytoplasm and nucleus is a topic of major interest in recent years [110]. Entropically less-stable heterogeneous phase-separated states are expected to become more stable than the entropically favorable homogeneous single phase, indicating that there is an enthalpic contribution by factors such as solute-solute interactions that maintain the stability of the phase-separated state [5]. Membrane-less organelles, commonly referred to as droplets, concentrates, or granules, differentiate from typical organelles in that they lack membranes [111, 112, 113, 114, 115]. Membrane-less organelles are formed through reversible processes that are sensitive to various external signals associated with cellular stressors [106, 116], as opposed to biomolecule aggregation which is generally irreversible [117]. The interface between the separated liquid-liquid phases has no partition barrier; this enables water molecules and solutes to pass freely through the interface such that droplets can dynamically exchange contentes with the external environment [118, 119]. It has been previously shown that droplets can be formed by cationic peptides and mononucleotides in laboratory conditions [120], additionally, droplets formed in cells often contain polyions such as cationic proteins and RNAs [121]. Numerous droplets have been identified within cells, each serving a biological function: the nucleolus [122], paraspeckles [123], nuclear speckles [112], Cajal bodies [113], and promyelocytic leukemia PML bodies [124]. These droplets perform many cellular functions, such as storing RNA and transcriptional factors through droplet formation and dissolution in the nucleus, as well as regulation of gene expression. This apparent importance of LLPS and droplet formation within the highly crowded cellular environment beckons more systematic studies on the effects of macromolecular crowding on LLPS and droplet formation.

Goobes *et al.* found that PEG promotes phase separation to a higher extent than other inert polymers due to its spherical conformations [125]. It was proposed that crowding agents act as a metabolic buffer that significantly extends the range of particular, intracellular conditions under which interactions occur due to the crowding-mediated shift in binding equilibria toward association. Measurements were conducted via isothermal titration calorimetry (ITC) and UV melting experiments and indicated that crowding-induced effects are marginal under conditions that are known to favor association of DNA strands but become progressively larger when conditions deteriorate. They state that crowding-mediated effects were found to include enthalpy terms that favorably contribute to association processes. It has been determined that processes that reduce excluded volume are entropically favored and therefore preferentially promoted in crowded environments [126, 66, 127, 128, 74]. Thus, processes leading to macromolecular compaction, such as DNA packaging, association and aggregation of polymers, formation of tight oligomeric structures, and folding of extended polypeptides, are significantly enhanced in the crowded cellular environment [129]. There have been a great many studies that have demonstrated that the crowding-mediated preference for maximizing compaction represents intracellular interactions that act to stimulate association between biopolymers and modulation of reaction rates [127, 128, 66, 130, 131, 132]. The thermal stability of long dsDNA structures has been shown to increase when crowded with inert polymers such as PEG or dextran [133], Goobes *et al.* found that short DNA strands behave similarly. The addition of PEG raised the dsDNA melting point by 4°C, and had similar results for dsDNA molecules containing one or two mismatched base pairs. Dextran 70 also increased the melting point for dsDNA, but not as effectively as PEG, showing only a 2°C increase in the melting point. The fact that neutral polymers enhance the thermal stability of relatively short dsDNA segments is of interest, because in contrast to long DNA molecules that tend to undergo collapse and aggregation in the presence of

PEG, short segments remain completely soluble. In the presence of inert polymers, the thermal stability of triple-stranded DNA is enhanced to a more significant extent than dsDNA molecules of comparable length [134, 135]. Triplex stabilization was enhanced by both PEG and dextran70, but significantly more-so by PEG. Additionally, Goobes *et al.* observed that triplex motifs containing mismatched bases are also effectively stabilized by PEG; the magnitude of the PEG-mediated increase of the triplex melting temperature was found to be constant and independent of the number of mismatched bases in the triplex motif. Throughout these measurements, various weights and concentrations of PEG were used. Concentrations were investigated over a range of 0-15% and a linear increase in melting temperature was observed for both dsDNA and triplex-DNA. PEG samples with concentrations greater than 15% were unable to be examined due to the increased viscosity. The correlation between the size of PEG polymers and the thermal stability of DNA species showed a slight improvement from PEG200 to PEG1000, but the effects of size were negligible from PEG1000 to PEG 8000.

2.4 Protein-DNA interactions

Another area of interest when investigating the effects of macromolecular crowders on DNA is protein-DNA interactions. Proteins are macromolecules consisting of one or more long chains of amino acid residues, they perform a wide variety of functions within organisms such as catalyzing metabolic reactions, DNA replication, providing structure to cells, transporting molecules, and responding to stimuli. There are many potential ways macromolecular crowders could affect the interactions between proteins and DNA, for example by volume exclusion effects such as trapping, caging or depletion forces, or by electrostatic effects which could lead to screening of charged proteins.

2.4.1 Nucleoid-associated proteins

Cristofalo *et al.* conducted magnetic tweezer (MT) experiments to observe the effects of polyethylene glycol on the affinity of DNA for the nucleoid protein H-NS and found that there were cooperative effects on the compaction of DNA fragments by H-NS and PEG [21]. Macromolecular crowding in a cell affects both the cytoplasm and chromosomal dynamics [136, 137, 138, 139], by influencing chromosome compaction through depletion-like interactions, as previously hypothesized [140, 39], and later observed [141, 142, 143]. Nucleoid-associated proteins (NAPs) can induce DNA condensation and modify chromosome organization by directly interacting with binding sites along the DNA [144, 145, 146, 147]. NAPs recognize binding sites at different levels of specificity, within the range of 10-30 bps [148], and can interact with DNA by different binding mechanisms (bending, bridging, or wrapping the double helix). Many NAPs stay bound for relatively long amounts of time [149, 150, 151, 152]. Studies on purified nucleoids with tuned concentrations of macromolecular crowders that do not bind or interact directly with DNA such as PEG have shown there is a complicated interplay between NAPs and crowders [153, 40, 42, 48]. H-NS is abundant and widespread in bacteria, having approximately 20,000 molecules per cell ($\sim 20\mu M$), is small in size, with a molecular weight of 15.5 kDa. H-NS is comprised of a C-terminal DNA- binding domain, and an N-terminal dimerization domain connected via a flexible linker [24, 154, 155, 156, 157]. The two interaction surfaces possessed by H-NS allows it to form attachments with neighboring proteins bound along the same DNA molecule that can result in stabilization of DNA loops [156, 158]. H-NS binds nonspecifically with DNA, although it is known to favor regions with more AT nucleotides [159, 160, 161, 162]. Cristofalo *et al.* used a MT setup to investigate the DNA extension while subject to externally applied forces, in the presence of both H-NS, and crowding via various concentrations of PEG1500. It was found that the critical points for DNA condensation in the presence of H-NS and PEG alone

are qualitatively different. In further experiments, they found that the presence of both H-NS and PEG triggers cooperative effects; after investigating the individual behaviors of DNA extension in the presence of H-NS or PEG alone, the combined effects of the NAP protein and the macromolecular crowder on DNA condensation were studied. The experimental conditions used in these measurements were chosen to be similar to those found in the cellular environment, where the volume fraction of proteins is reported to be between 12 and 17% [150], and solute molecules take up 30 to 40% [18, 11, 8, 10, 7, 12].

Lin *et al.* conducted investigations into a different NAP, HU (Histone-like protein from strain U93) [163]. HU is a NAP expressed in most eubacteria with tens of thousands of copies; it is believed to organize and compact DNA via binding, and is one of the most abundant proteins in *E. coli* cells [164]. It was reported that DNA binding properties on HU were influenced by both macromolecular crowding and salt conditions. Three different crowders were used in this investigations: blotting grade blocker (BGB), bovine serum albumin (BSA), and PEG8000; as well as two different $MgCl_2$ concentrations in an effort to mimic the intracellular environment. BGB is a non-fat milk-product mixture comprised mostly of casein micelles containing large globular proteins ranging from 50 to 600 nm in diameter [165, 166]. Investigating the effects of magnesium ions was of interest because of their crucial role in the functionality of many proteins and enzymes [167, 168, 169, 170, 171, 172]. Measurements were conducted via tethered particle motion (TPM), where DNA is attached to a substrate on one end, while the other is attached to an observable bead subject to Brownian motion. Two binding regimes are observed, with a transition between them, compaction and extension of the HU protein. These regimes were found to be highly sensitive to crowding conditions. The observations suggest that magnesium ions enhance the compaction of HU-DNA and suppress filamentation, while BGB and BSA increase the local concentration of the HU protein by more than 4-fold, and seem to

suppress filament formation. They did report that PEG8000 was not a good crowding agent under these experimental conditions for concentrations above 9% (w/v), due to potential interactions with DNA, HU, and/or surfaces. The latter may explain why PEG can instead be more easily used as a crowder in MT measurements. Experiments were conducted via titration from 0 to 1600 nM HU under the following crowding conditions: 0.5% and 1% BGB, 1.25%, 5% and 10% BSA, 3%, 9%, 15% PEG8000 in the buffer without $MgCl_2$, and 0.5% BGB, 10% BSA, and 3% PEG8000 in the buffer containing $MgCl_2$, where all percents are (w/v) of the crowding agent. It was found that BGB increases local HU concentration, stimulating HU binding and the subsequent DNA bending at significantly lower HU concentrations; from 150 nM HU in the uncrowded buffer without $MgCl_2$ to 12.5 nM HU in both BGB crowding environments. In the absence of $MgCl_2$, there were some notable differences between the 0.5% and the 1% (w/v) BGB; maximal DNA compaction occurs at a lower HU concentration in the low BGB concentration compared the higher BGB concentration (25 nM versus 100 nM HU). This observation implies a balance between crowding effects on binding energy and on diffusion; the authors suggest that too much crowding by BGB might hinder HU access to DNA. It was also observed that at higher HU concentrations where HU forms filaments along the DNA, the root-mean-square (RMS) increases less in the presence of BGB than in conditions without BGB. Additionally, the impact on filament formation in 1% BGB was observed to be stronger than in 0.5% BGB, suggesting that BGB inhibits HU filamentation. In the presence of $MgCl_2$, the RMS was reduced an additional 7% compared to the RMS without BGB. Given that the compaction of DNA by HU in the presence of $MgCl_2$ was already enhanced without BGB, it was concluded that $MgCl_2$ and BGB exhibit cooperative dynamics that enhance DNA compaction. It was also observed that BSA increased local HU concentration. Three concentrations of BSA (1.25%, 5%, and 10% (w/v)) in the absence of $MgCl_2$, and 10% BSA in the presence of $MgCl_2$ were used to investigate

the effects of BSA on HU binding. The compaction and de-compaction of DNA was observed across a wider concentration range in the presence of BSA, when compared to the absence of BSA. Compaction was observed at 6.25 nM HU in 1.25% and 5% BSA, and at 12.5 nM HU in 10% BSA, while in the case without BSA the compaction was observed at 150 nM HU. These observerations suggest that BSA increases the local concentration of HU dimer and lead the Lin *et al.* to conclude the following: the most compact state attained in the presence of BSA does not show a significant difference compared to that in the absence of BSA (the minimum RMS of the DNA was approximately constant through all measurements), too high of a concentration of BSA is less effective in increasing the local HU concentration [163]. Similarly to the crowding with BGB, too much crowding with BSA might interfere with HU binding; possibly interacting with the HU and/or the DNA [173], or via steric effects. They next observed the effects of BSA in the presence of $MgCl_2$, and found that the most compact state of the DNA occurred at a higher concentration of HU dimer. This observation is unable to be explained by the impact of $MgCl_2$ or BSA individually. The impact of PEG8000 on HU binding was also investigated in this study using three concentrations of PEG8000 (3%, 9%, and 15% (w/v)) in the absence of $MgCl_2$, and 3% PEG8000 in the presence of $MgCl_2$. It was found that compaction starts at 12.5 nm HU in 15% PEG8000, 50 nm HU in 9% PEG8000, and 100 nM HU in 3% PEG8000, as opposed to the 150 nM HU required for compaction in the crowding-free condition, suggesting that relatively high concentrations of PEG8000 is needed in order to increase local HU concentration. Additionally, there were no significant effect on the value of the lowest RMS for the 3% and the 9% PEG8000, while 15% PEG8000 demonstrated a dramatic 30% decrease in the RMS of the DNA compared to the crowder-free condition. In the presence of $MgCl_2$, the most compact state for 3% PEG8000 and 8mM $MgCl_2$ occured at 100 nM HU and showed a 7% reduction in the RMS when compared to the RMS of the DNA in the presence of $MgCl_2$ in the

absence of PEG8000. It was observed that the most compact state of the DNA in the absence of $MgCl_2$ did not change regardless of the PEG8000 concentration, suggesting that $MgCl_2$ works cooperatively with PEG8000 to enhance DNA compaction [163].

2.5 Theoretical works on effects of macromolecular crowders on polymers

Cao *et al.* conducted Langevin simulations to investigate the conformational change of a semi-flexible chain in a concentrated solution packed with spherical active crowders [4]. They observed that a novel shrinkage-to-swelling transition is observed for polymers with small rigidity. A phase diagram was constructed in the parameter space of active force and crowder size; the variation of the polymer gyration radius exhibited a non-monotonic dependence on the dynamical persistence length of the active particle. Information was also elucidated about the activity-crowding coupling effect in different crowder size baths. It was determined that for small crowders, activity increases the crowding-induced shrinkage to the chain, while as crowder size is increased, activity begins to hinder the crowding effects resulting in a competitive shrinkage and swelling of the polymer chains. For large crowders, the swelling effect from activity dominates the crowding effects.

Sapir and Harries conducted several theoretical investigations in attempts to explain the effects observed in crowded environments [174, 175, 176], as well as the investigation they conducted with Sukenik [177]. The Sukenik *et al.* paper reviewed the origins of the effective attractive interactions that emerge between and within macromolecules immersed in solutions containing cosolutes that are preferentially excluded from the macromolecular interfaces [177]. They summarized that for many polymers at low to moderate concentrations the steric interactions and molecular crowding effects dominate, and cosolutes primarily act through entropic

mechanisms. On the other hand, for small excluded solutes such as naturally occuring osmolytes processes are dominated by primarily favorable enthalpy mechanisms. They also investigated whether the depletion force was entropic [176]. They used the Asakura-Oosawa model and the Kirkwood-Buff solution theory to describe the effects of cosolutes frequently excluded from molecular crowding investigations. They reviewed experimentally found mechanisms and linked those to possible underlying molecular interactions. Cosolutes such as osmolytes, tend to induce attractive depletion forces that are enthalpically dominated and entropically destabilizing, while polymeric crowders may act by similar mechanisms but often induce depletion forces dominated by favorable entropy. The Asakura-Oosawa model for depletion forces assumes a completely steric cosolute-macromolecule interaction, leading to fully entropic depletion forces. Sapir and Harries altered the steric repulsion core with a 'soft' repulsive shell that adds an enthalpic contribution to the depletion force. Considering that the cosolute-macromolecule interactions are temperature-dependent yields a depletion force that can be tuned to favor enthalpy over entropy. According to Sapir and Harries, these simple considerations regarding the nature of the cosolute-macromolecule effective interaction can be used to rationalize the complete range of cosolute effects.

The next investigation from Sapir and Harries provided a mean field theory for crowded solutions [174]. Their proposed mean field theory to account for experimentally determined temperature dependence of protein stabilization that emerges in solutions crowded by preferentially excluded cosolutes. They employed the Flory-Huggins approximation to regular solution theory to come up with a model that describes cosolutes in terms of their size, and two temperature-dependent microscopic parameters that correspond to cosolute-macromolecule and bulk solution interactions. This theory was able to predict a 'depletion force' that was able to account for experimentally observed stabilization in protein folding or association in the presence

of excluded cosolutes. Additionally, the theory also predicts the full range of associated entropic and enthalpic components. This theory describes entropically as well as enthalpically dominated depletion forces, even those disfavored by entropy, in accordance with experiments and depending on specific cosolutes. The depletion attraction that emerges through this theory is not simply described by molecular volumes, but by an effective volume instead. This effective volume represents an interplay between solvent, cosolute, and macromolecular interactions. They began with examining the mean field theory of cosolute solutions (MFC) in the limit of the Asakura and Oosawa model (AOM) [178, 179]. In the AOM, interactions of cosolutes with the surface is purely steric and other interactions are omitted, and for an ideal solution. For an ideal cosolute-solvent solution lacking nonideal mixing terms, the only remaining relevant parameters are the cosolute size and the parameters quantifying the cosolute interaction with the interface. This causes a deviation from the AOM prediction that is explained as describing an "effective" volume as opposed to the excluded volume.

Shin *et al.* conducted Monte Carlo simulations to investigate and found that large crowders lead to caging of the polymer, while small polymers tend to mix with the chain monomers and increase the effective viscosity [180]. The main focus of this study was to investigate the kinetics of polymer looping with macromolecular crowders; specifically they wanted to look into the effects of volume fraction and crowder size. The looping dynamics of flexible polymer chains in the presence of different degrees of crowding was investigated in detail. By analyzing the looping-unlooping rates and looping probabilities of the chain ends it was shown that small crowders typically slow down the chain dynamics, while larger crowders seem to facilitate the looping. These observed effects are explained in terms of an effective solution viscosity and standard excluded volume; they were able to show that for small crowders the effect of an increased viscosity dominates, while for larger crowders confinement effects drive dynamics.

Chapter 3

Effects of macromolecular crowding on LacI-mediated looping in DNA

3.1 Introduction

Deoxyribonucleic acid (DNA) is an organic polymer that encodes up to tens of thousands of genes, and is highly compacted within cells. In some cases, the linear length of DNA that is compacted inside is as much as a million times the length of a cell [181, 182, 183, 184, 185, 186, 187, 188, 189, 190, 191]. DNA compacts through protein-mediated topologies, such as loops, as well as supercoiling [192, 193, 194]. Indeed, proteins, like the lac repressor (LacI), alter DNA topology by mediating long-range loop formation [195]. Protein-mediated DNA looping can occur in two different conformations, parallel and anti-parallel, with the anti-parallel conformation requiring a larger length of DNA to form the loop [196]. The cellular environment is highly crowded, with *E. coli* cells having 30-40% of the volume taken up by crowders, which are the various macromolecules contained within the cell [11, 10, 7, 8, 12]. Due to the highly crowded nature of the cellular environment, and the ability of LacI to create loops in DNA, I set out to investigate the effects of macromolecular crowding

on protein-mediated looping in DNA.

3.1.1 DNA structure

The organic polymer DNA is constructed of two anti-parallel polynucleotide chains that coil around each other in a double helix. Each chain is composed of a sequence of deoxyribonucleotides containing four different bases: Adenine (A), Guanine (G), Thymine (T), or Cytosine (C). The double helix structure of DNA is stabilized by stacking interactions and hydrogen bonds (H-bonds) formed between bases bridging the two chains, according to base pairing rules (A pairs with T through two H-bonds, C pairs with G through three H-bonds). The most common form of DNA is *B*-DNA, where the double helix is wound with a right-handed chirality [197].

3.1.2 *lac* repressor (LacI) and LacI mediated looping

The lac repressor (LacI) is a DNA binding protein that binds to specific DNA sequences (operators). LacI is produced in order to repress the expression of the lac operon (a specific sequence of three genes that control the metabolism of lactose in *E. coli*) by binding to the O1 operator, which slightly overlaps the operon promoter. Lac repressor is a homo-tetramer formed of two pairs of dimers that interact via their C-terminal domains (CTDs), forming a V shape. The ends of the V contain DNA binding N-terminal domains (NTD). Each end of the V is able to simultaneously bind to an operator, causing DNA to loop. There are four types of operators with different binding affinities for LacI, which in order of binding affinities are: the synthetic "Oid", and the naturally occuring "O1", "O2", and "O3". A cartoon schematic of the LacI structure is shown in Fig. 3.1.

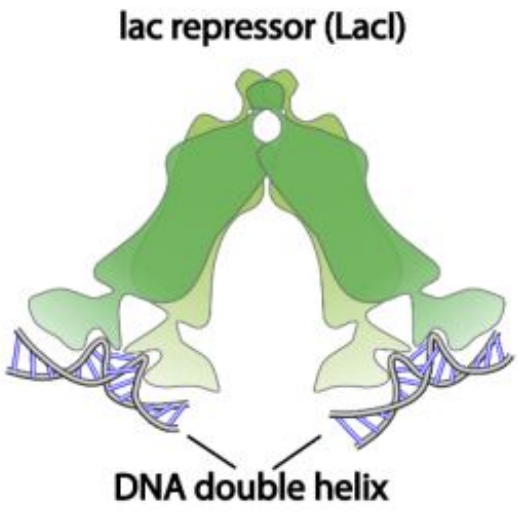

Figure 3.1: Cartoon of LacI tetramer bound to two DNA operators. Figure reproduced with permission from Xu (2022) [1].

3.2 Materials and methods

3.2.1 DNA preparation

The DNA fragments used in all my experiments were produced by Polymerase Chain Reaction (PCR). The reaction mixture contains the plasmid of choice, primers (eurofins Genomics) designed using "A plasmid Editor" (ApE) [198], deoxynucleotide triphosphates (New England BioLabs, NEB), Taq/Q5 DNA polymerase (NEB), the appropriate buffer and nuclease-free water. Biotin- and digoxigenin-labeled DNA fragments were utilized for tethered particle motion experiments (TPM), with one end attached to a substrate, and the other to a bead.

3.2.2 Chamber preparation

The bottom coverslip (Fisherbrand, Thermo Fisher Scientific, Waltham, MA, USA) used to construct the microchamber supports a parafilm gasket that is cut to shape with a laser cutter (Universal Laser Systems, VLS 860, Middletown, CT, USA) with a

central observation section connected via narrow channels to inlet and outlet reservoirs just beyond the edges of the top coverslip. Once the chamber is assembled it, is heated to approximately 85° C on a hotplate to seal the components together and finish the microchamber. The narrow inlet and outlet help to reduce the evaporation of the buffer solution inside the chamber, and the triangular observation section restricted the volume to approximately 6 μL and provided a gradient of tether densities to optimize the utility of chambers.

The buffer used differed slightly between projects. Phosphate buffered saline (PBS) and λ buffer (10mM Tris-HCl (pH 7.4), 200/100 mM KCl, 5% DMSO, 0.1 mM EDTA, 0.1 mg/mL α-casin, 0.2 mM DTT) were used in LacI-mediated DNA looping experiments (discussed in this chapter). A buffer comprised of 10 mM Tris-HCl pH 7.4, 1 mM $MgCl_2$, 0.5 mM ATP/AMP-PNP, 1 mM DTT was used for KIF4a compaction experiments (discussed in Chapter 3). The entire sample preparation was conducted at room temperature ($\sim$20° C) and materials were kept on ice. The beads used in TPM measurements were 0.32 μm in diameter, streptavidin-coated polystyrene beads (Spherotech, Lake Forest, IL, USA).

Chambers were incubated with 10 μL anti-digoxigenin at a concentration of 5 μg/mL (Roche Life Science, Indianapolis, IN, USA) in PBS at room temperature for 1 hour. The anti-digoxigenin was then rinsed out with PBS and the chambers were then passivated with West-EZ Blocking Buffer (25 mM Tris-HCl pH 7.4, 150 mM NaCl, 1% α-casin (w/v)) (GenDEPOT, Katy, TX, USA) for 30 min. DNA tethers in λ buffer were then incubated in the chamber for 15 min to be anchored through a single digoxigenin to the anti-digoxigenin-coated coverslip. The other end of the DNA was anchored to a streptavidin-coated bead via a single biotin by adding 0.03 mg/mL beads solution in λ buffer for a 15 min incubation. Excess, untethered beads were then flushed out of the chamber with 120 μL of λ buffer. Beads were washed thrice in PBS and once in λ buffer before being resuspended in λ buffer prior to being

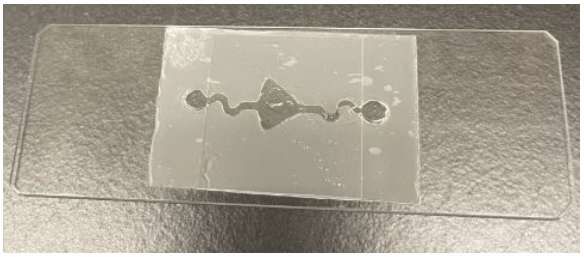

Figure 3.2: Image of a microchamber used in experiments. A parafilm gasket is sandwiched inbetween a large bottom coverslip and a smaller top coverslip that leaves the narrow inlet and outlet reservoirs exposed. The chamber is heated until sealed with a total volume of approximately 6 μL.

introduced to the chamber. An image of a typical microchamber is shown in Fig. 3.2.

3.2.3 Proteins

LacI was provided by Kathleen Matthews (Rice University). KIF4a (discussed in Chapter 3) was provided by Radhika Subramanian (Harvard University).

3.2.4 Tethered particle motion (TPM) microscopy

Tethered particle motion (TPM) microscopy is a quite powerful, yet simple tool for quantitative analysis of individual polymer tethers (DNA in this case) and their interactions with various entities (proteins in this case). Microspheres undergo Brownian motion while tethered to a glass substrate by an individual polymer. The bead diffuses throughout a hemisphere, the size of which is dictated by the tether length. The scatter of positions of the tethered microsphere in the XY plane is recorded to identify the anchor point and the extent of excursions around it. The excursion amplitude, ρ, value can be converted to the effective tether length using an appropriate calibration curve.

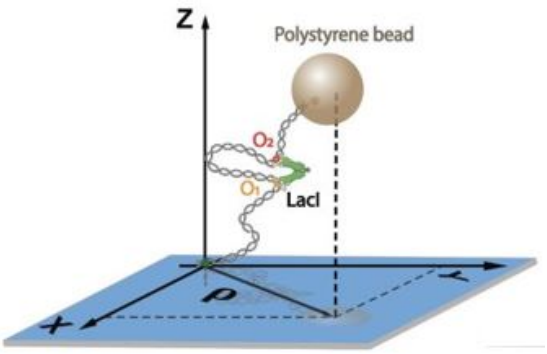

Figure 3.3: Cartoon of the TPM experimental setup. One end of the DNA tether is anchored to a glass substrate while the other is attached to a polystyrene bead that is subject to Brownian motion. Figure reproduced with permission from Xu (2022) [1].

3.2.5 TPM microscope

The microscope (Leica DM LB-100, Leica Microsystems, Wetzlar, Germany) (shown in Fig. 3.4) I used is fitted with an oil-immersion objective (N-Plan 100 × 1.4) and a CV-A60 CCD camera (JAI, Copenhagen, Denmark). The video sequence was digitized using an IMAQ PCI-1409 frame grabber (National Instruments, Austin, TX) and analyzed using a custom LabVIEW (National Instruments, Austin, TX) program. In order to avoid blurring, the exposure time of the CCD camera was minimized. The exposure needed to be significantly quicker than the time, t_b, required for the bead to traverse its full excursion. A rough estimate is given by $t_b = \sigma^2/D$, where σ is the range of motion and D≈1000 nm^2/ms is the diffusion coefficient of the bead obtained via the Stokes-Einstein relation. Typical values for t_b are roughly 50 ms so I used exposures of 1 ms to ensure the exposures are safely lower than t_b. The video camera used an interlaced format such that the even lines of each image are exposed 20 ms after the odd lines. I analyzed the even and odd fields as independent sequences in order to avoid blurring from this 20 ms offset. This effectively doubled the pixel spacing in the vertical direction from 64 to 128 nm in the field of view, but had no significant effect my determination of bead positions.

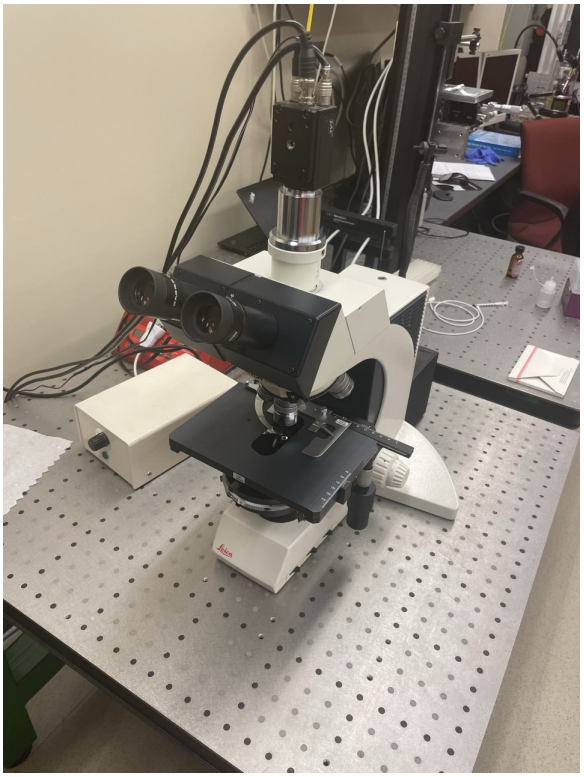

Figure 3.4: Photograph of the TPM microscope in the Finzi-Dunlap lab used for the measurements described in this dissertation.

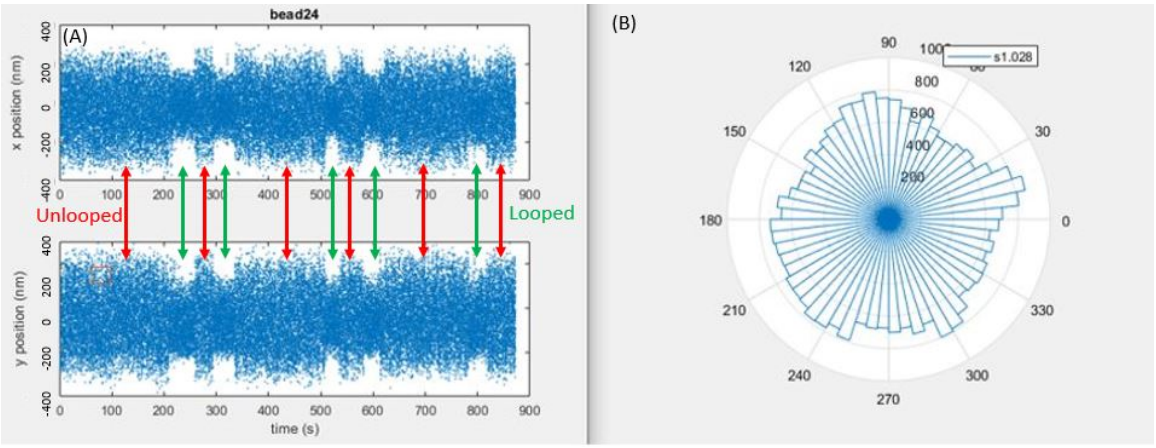

Figure 3.5: Representative trace of a bead showing looping. (A) Data of the x and y positions of a representative bead as a function of time. Areas with lower excursion are looping events. (B) Results of symmetry test for this representative bead.

3.2.6 TPM data collection and analysis

The XY position of each bead was recorded at 50 Hz interlaced with a custom LabVIEW (National Instruments, Austin, TX, USA) program. Vibrational or mechanical drift in the position of each bead was eliminated by subtracting the average location of reference beads that were adhered to the substrate within the same field of view [199, 200, 201]. The effective length of each tether was then calculated as $< \rho >_{8s} = < \sqrt{(x - < x >_{8s})^2 + (y - < y >_{8s})^2} >_{8s}$, in which $< x >_{8s}$ and $< y >_{8s}$ are eight-second moving averages representing the coordinates of the anchor point of a bead. The anchor point is determined by finding these average x and y positions. Changes in the effective DNA tether length are represented as changes in the excursion length of the bead [202, 203, 204]. Any beads with (x, y) position distributions with a ratio of the major to minor axes greater than 1.07 were discarded to exclude beads tethered by multiple DNA molecules [201]. Excursion data from the time records of beads, in the same experimental conditions, which passed the "symmetry test" were retained for the analysis described below.

The excursion data was summarized in histograms that in the presence of LacI, dis-

played three peaks indicating a parallel looped conformation, an anti-parallel looped conformation, and the unlooped state [205]. The histograms were then visually checked to ensure the three peaks were in appropriate locations corresponding to each of the three possible tether conformations. Once proper peak locations were verified and data displaying extraneous peaks were discarded, the excursion data was analyzed, by fitting the data with a function composed of a sequence of steps between the different excursion levels. For each individual trace, data where the bead remained in one state for more than 50s was discarded as some beads would appear to 'lose the ability to loop,' most likely due to a second lac repressor binding to the O2 operator, saturating the DNA molecule's ability to bind to LacI and therefore form loops. Error analysis was conducted via a 100 batch bootstrapping of samples including 1/3 of the entire dataset.

The data was initially analyzed by fitting Gaussians to the cumulative histograms of the data and using the area under the peaks to determine the probability of the tether being in any given conformation. The issue with this Gaussian fitting was that the two looped conformations are so close to each other, that the Gaussians would overlap such that identical values would be associated with different levels, leading to inaccurate reporting of probabilities, which is why the previously described method of data analysis was used. The analyzed data in Fig. 3.6, shows that the addition of macromolecular crowders causes DNA to prefer the parallel conformation over the anti-parallel conformation, while leaving the probability of the unlooped conformation relatively unchanged. One potential explanation for this is that the addition of macromolecular crowders decreases the 'goodness' of the solvent causing the polymer (DNA in this case) to favor self-interaction. Separate evidence for this explanation is that often as crowder concentration was increased, beads tended to adhere to the surface of the substrate, which might have been caused by DNA forming compact globules. Additionally, it is shown that for 100 mM KCl, we see a drastic decrease

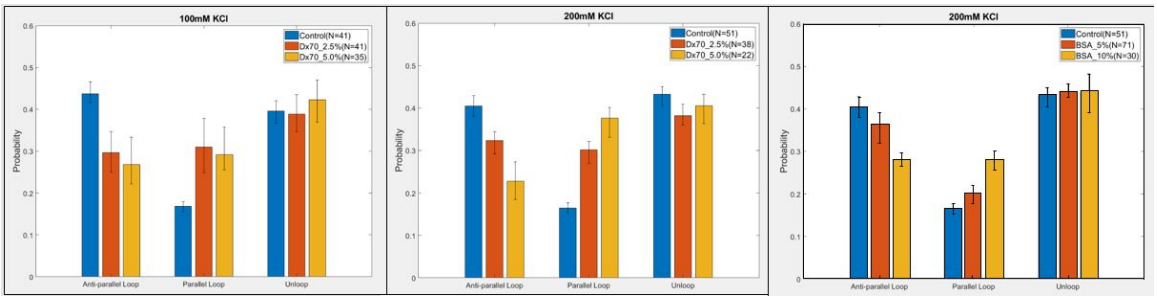

Figure 3.6: Bar graph showing the probabilities of the anti-parallel, parallel, and unlooped conformations under various salt and crowding conditions. N is the number of beads for which data was included, $Dx70\_2.5\%$ corresponds to a 2.5% (w/v) of dextran 70, this notation is consistent for $Dx70\_5.0\%$, and the BSA data. The error bars were determined via a 100 batch bootstrapping of samples including 1/3 of the entire dataset.

in the anti-parallel loop conformation at lower levels of crowding than compared to what we see for 200 mM KCl.

3.3 Discussion and conclusion

Although the cellular environment is highly crowded, up to 40%, most *in vitro* experiments occur in a dilute buffer. In order to bridge the gap between *in vitro* and *in vivo* measurements, I added macromolecular crowders to laboratory measurements of protein-mediated looping of DNA. I observed that the addition of macromolecular crowders caused DNA to favor the parallel loop conformation over the anti-parallel loop conformation, while the probability of the DNA being unlooped remained relatively constant. These effects were more prominent in a buffer with 100 mM KCl than they were for 200 mM KCl. These levels of salt were chosen because they are physiologically relevant, being similar to the 130-145 mM of NaCl found extracellularly inside the human body [206], and KCl was used in these experiments because potassium is more concentrated inside the cell.

Chapter 4

hKIF4a compaction of DNA

4.1 Introduction to hKIF4a

hKIF4a is a chromokinesin, a member of a kinesin protein family which contains a specific DNA binding domain, and are microtubule-motor molecules that display chromatin binding activity and play a key role in mitotic and meiotic regulation [207, 208, 209]. Kinesins ar adenosine triphosphate (ATP)-dependent mechanochemical motor involved in the transportation of cytoplasmic cargo along microtubule fibers. "ATP is an organic compound and hydrotrope the main function of wihch is to provide energy to drive a variety of processes in living cells. When ATP is consumed through metabolic processes, it is converted to either adenosine diphosphate (ADP) or to adenosine monophosphate (AMP). ATP is regenerated within the human body to such an extent that the human body recycles its own body weight in ATP daily" [210, 211]. ATP is classified as a nucleoside triphosphate, meaning that it consists of a nitrogenous base (adenine), a sugar (ribose), and a triphosphate [210, 211]. Kinesins are involved with spindle assembly, microtubule attachment at the kinetochores, which are protein structures associated with duplicated chromatids, chromosome alignment and condensation, and cytokinesis [207, 212, 213, 214]. Chromoki-

nesins are distinct due to their ability to associate with chromosomes during mitosis. hKIF4a is a member of kinesin 4 family that participates in various aspects of mitosis [208]. Mitosis is the process through which a cell replicates its chromosomes and then separates them, producing two identical nuclei prior to cell division. Mitosis is typically followed by equal division of the genomic content of cells into two identical daughter cells with identical genomes. All eukaryotic cells prepare for cell division via formation of a "mitotic spindle," which is a bipolar machine constructed of microtubules and many associated proteins. This mitotic spindle organizes previously duplicated DNA such that one copy of each chromosome attaches to each end of the spindle. Both the formation and the function of the spindle requires very precise microtubule dynamics, as well as multiple motor enzyme mechanics [215]. hKIF4a is a unique member of this group that localizes to the nucleus during interphase of the cell cycle. Additionally, hKIF4a has been found to associate with the breast cancer susceptibility gene product BRCA2 [207]. In the absence of hKIF4a, chormosomes become overcondensed and shorten their axes [216].

4.2 hKIF4a utilizes ATP to compact DNA

AMP-PNP is a non-hydrolysable analogue of ATP that inhibits fast axonal transport and facilitates the interaction between membranous organelles and microtubules [217]. For measurements, a chamber of DNA tethers attached to beads were prepared for TPM as described in Chapter 2, using a buffer comprised of 10 mM Tris-HCl pH 7.4, 1 mM $MgCl_2$, 0.5 mM ATP, and 1 mM DTT. Initial measurements were conducted in chambers with bare DNA (no hKIF4a), as well as a truncated variety of hKIF4a without the DNA binding domains. As shown in the cumulative histograms and individual traces, the bare DNA (Fig. 4.1) and the truncated protein (Fig. 4.2) were indistinguishable, both having average ρ values of approximately 150 nm well

clustered and values in the probability distribution function (PDF) around $\sim 1.4 \times 10^{-3}$.

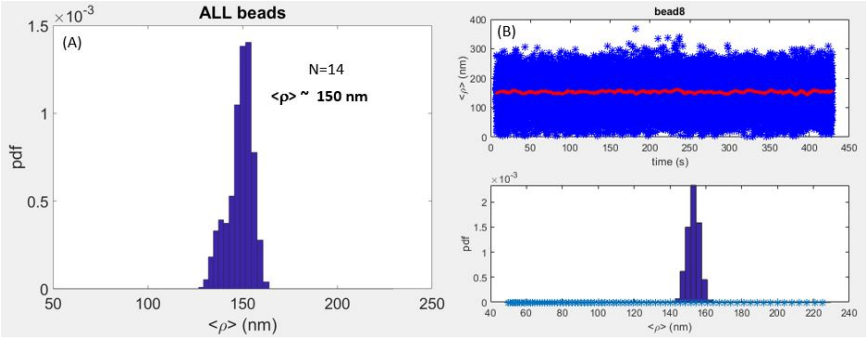

Figure 4.1: (A) Cumulative histogram for measurements in buffer solution in the absence of hKIF4a. (B) Representative trace of a tethered bead attached to bare DNA. Tethers in this solution had an average 2D excursion of 150 nm.

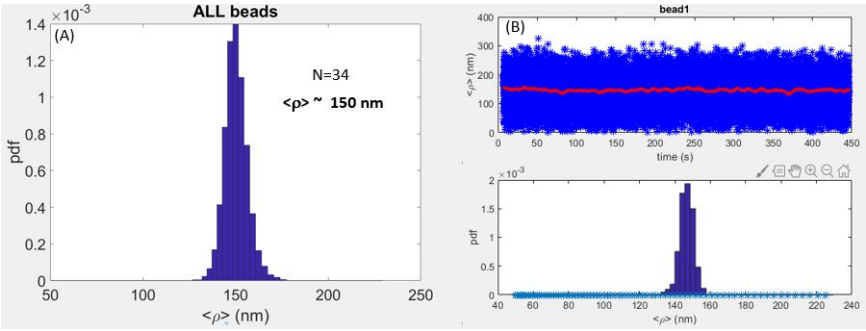

Figure 4.2: (A) Cumulative histogram for measurements in buffer solution with a truncated version of the hKIF4a protein (50 nM) that is not expected to bind to DNA. (B) Representative trace of a tethered bead in the presence of truncated hKIF4a. Tethered beads exhibited an average excursion of 150 nm, consistent with bare DNA.

Measurements with full length hKIF4a were conducted using 50 or 10 nM hKIF4a; 50 nM showed a greater extent of compaction as compared to 10 nM hKIF4a. Measurements were conducted with 0.5 mM ATP or AMP-PNP. Under both concentrations of hKIF4a, ATP yielded significantly higher levels of compaction compared to

AMP-PNP, as shown in Fig. 4.3 and Fig. 4.4. In the 10 nM case, the PDF value for the uncompacted peak had a value of $\sim 2.2 \times 10^{-4}$ with ATP, and $\sim 5 \times 10^{-4}$ with AMP-PNP, while with a concentration of 50 nM hKIF4a, the PDF values for the uncompacted peak were $\sim 1 \times 10^{-4}$ with ATP $\sim 3 \times 10^{-4}$ with AMP-PNP.

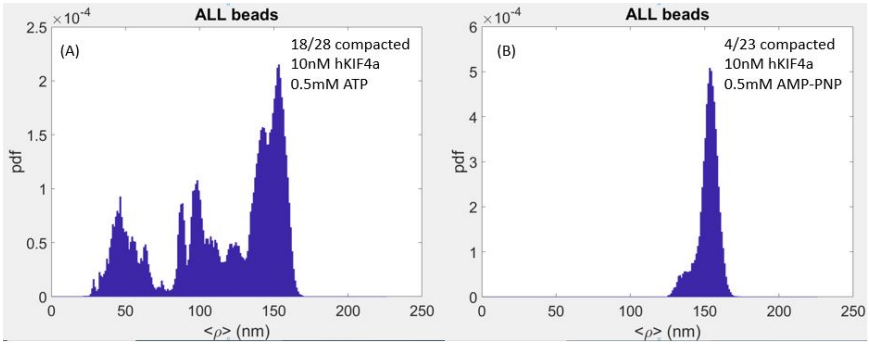

Figure 4.3: (A) Cumulative histogram for 10 nM hKIF4a, 0.5 mM ATP. Out of the 28 tethers included in this histogram, 28 showed compaction. (B) Cumulative histogram for 10 nM hKIF4a, 0.5 mM AMP-PNP. Out of the 23 tethers included in this histogram, only 4 showed compaction. Those four tethers showed a lesser extent of compaction than those exposed to ATP.

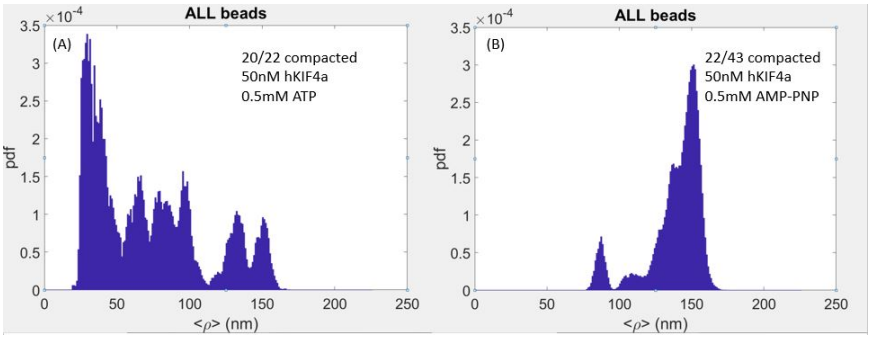

Figure 4.4: (A) Cumulative histogram for 50 nM hKIF4a, 0.5 mM ATP. Out of the 22 tethers included in this histogram, 20 showed compaction. (B) Cumulative histogram for 50 nM hKIF4a, 0.5 mM AMP-PNP. Out of the 43 tethers included in this histogram, only 22 showed compaction. The tethers that did show compaction showed a lesser extent of compaction than those exposed to ATP.

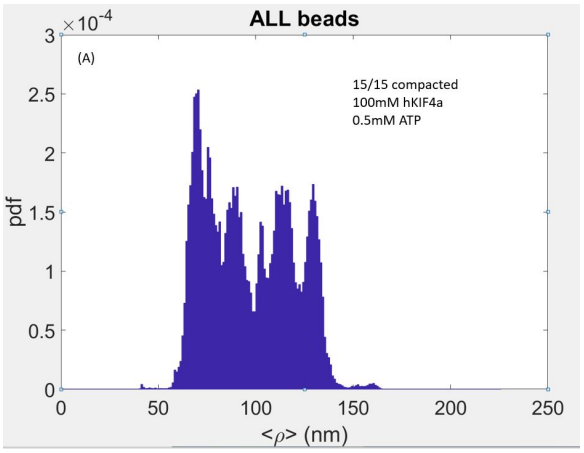

Figure 4.5: Cumulative histogram for 100 nM hKIF4a, 0.5 mM ATP. All 15 of the tethers included in this histogram showed compaction.

Additionally, measurements with higher concentrations of hKIF4a were conducted. Fig. 4.5 shows data for 100 nM hKIF4a with 0.5 mM ATP and in the same buffer condition as described above. Interestingly, all 15 tethers recorded showed compaction and the PDF value for the uncompacted peak on this histogram is nearly negligible, further supporting the idea that higher levels of hKIF4a lead to a higher extent of compaction. Measurements were also conducted with concentrations of 250 and 500 nM hKIF4a; in these concentrations, all beads adhered to the surface of the microchambers, suggesting that maximum compaction was attained. This observation of maximum compaction motivates future measurements with longer DNA tethers to elucidate information regarding the extent to which these concentrations of hKIF4a can compact DNA.

4.3 hKIF4a variation without ATPase compacts DNA

Upon observing that hKIF4a utilizes ATP to compact DNA, I was interested in seeing whether or not a variation of hKIF4a with the ATPase deleted would be able

to compact DNA. ATPases are a class of enzymes that catalyze the hydrolosis of a phosphate bond in ATP, decomposing it to ADP and a free phosphate ion [218]. These measurements were conducted with concentrations of 20 nM and 200 nM hKIF4a mutatant (Fig. 4.6), with the 20 nM case having a PDF value for the uncompacted peak of $\sim 2.7 \times 10^{-4}$, and the 200 nM case having a PDF value of $\sim 0.5 \times 10^{-4}$ This shows that the DNA binding sites alone enable hKIF4a to compact DNA. This, along with the data from Figs. 4.3 and 4.4, show that both the DNA binding sites, and the ATP-fueled motor domain contribute to the compaction of DNA.

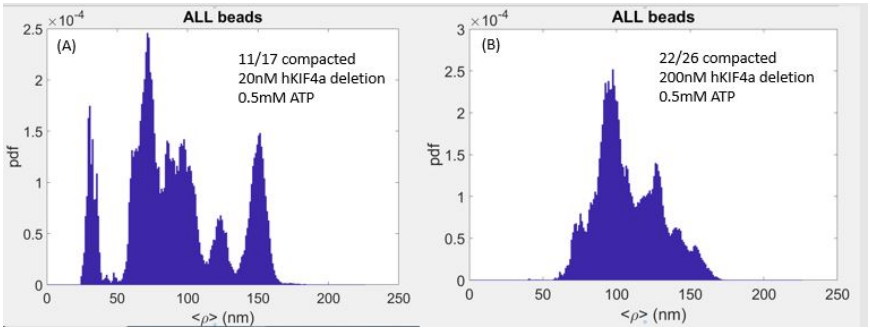

Figure 4.6: Cumulative histograms for variation of hKIF4a without ATPase. (A) Cumulative histogram for 20 nM hKIF4a mutation. Out of 17 tethers included in this histogram, 11 showed compaction. (B) Cumulative histogram for 200 nM hKIF4a mutation. Out of 26 tethers, 22 showed compaction.

4.4 BSA may aide hKIF4a in compaction of DNA

Next, I wanted to investigate the effects of crowding on hKIF4a-mediated compaction of DNA using BSA as a macromolecular crowder. These measurements were difficult due to both hKIF4a and BSA inducing sticking of beads to the surface of the microchamber. Control data is shown in Fig. 4.7, with 5% BSA (w/v) in the absence of hKIF4a. I was only able to record two beads throughout these measurements (Fig. 4.8), both of which showed a much greater level of compaction than the mea-

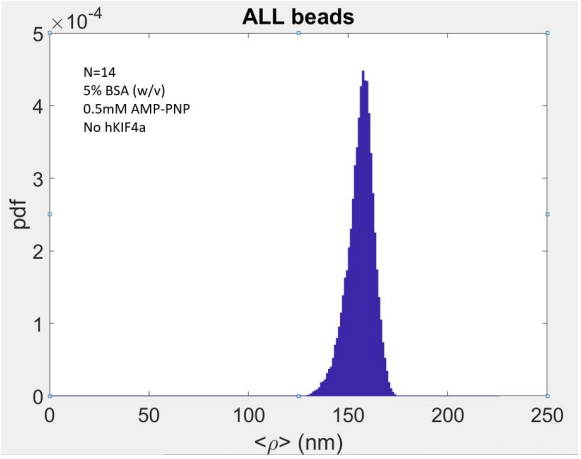

Figure 4.7: Control data for 5% BSA (w/v) in the absence of hKIF4a, no compaction is observed.

surements without BSA. The values for the uncompacted peak in the PDF were as follows, $\sim 4.5 \times 10^{-4}$ in the presence of BSA, but without hKIF4a, and $\sim 2 \times 10^{-4}$ in the presence of both BSA and hKIF4a. It is important to note that the PDF value reported from the histogram in the presence of both BSA and hKIF4a contains 600s of data prior to the addition of BSA and hKIF4a. These measurements were conducted with AMP-PNP, which yielded very little compaction in the absence of BSA. The first bead that was recorded, Fig. 4.8B, did not have either hKIF4a or BSA for the first 600s of the measurement. That first 600s is the only section of the cumulative histogram that does not show compaction. This is potentially evidence for the impact that macromolecular crowding could have during the cell cycle.

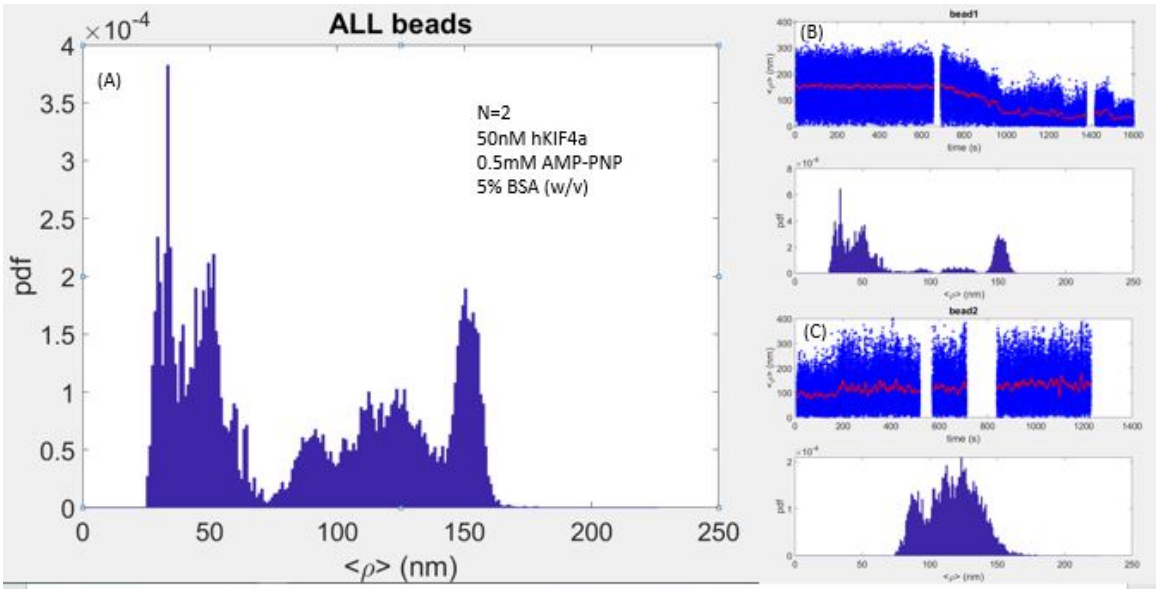

Figure 4.8: (A) Cumulative histogram for 50 nM hKIF4a, 0.5 mM AMP-PNP and 5% BSA (w/v). Only two tethers were able to be included in this histogram. This is because both hKIF4a and BSA induce sticking of beads inside the microchambers, making measurements difficult. Both beads that did not stick showed much higher levels of compaction than were observed in the BSA-free case. (B) A trace from a bead that did not have hKIF4a or BSA for the first 600s of the measurement, once hKIF4a and BSA were added to the chamber, immediate gradual compaction of the DNA was observed. (C) A trace during which hKIF4a and BSA were in the microchamber throughout the measurement.

4.5 Discussion and conclusions

hKIF4a is a protein that is of key importance to the cell cycle. Using TPM measurements, I have shown that hKIF4a compacts DNA, more-so with ATP than AMP-PNP. I found that ATP compacts almost twice as much as DNA tethers with AMP-PNP for 10 nM hKIF4a, and approximately three times as much for 50 nM hKIF4a. It

was also shown that 100 nM hKIF4a compacted every DNA tether to some degree, while 250 nM and 500 nM hKIF4a likely induced maximum compaction of DNA such that all tethers condensed full to the surface of microchambers. The possibility of maximum compaction of DNA by higher concentrations of hKIF4a motivates further experiments with longer DNA tethers. Measurements of a hKIF4a variation without ATPase showed that the DNA binding sites alone are able to compact DNA. It was also observed that through measurements with BSA that macromolecular crowding may strongly enhance the compaction of DNA via hKIF4a. It is currently difficult to quantify the effects of BSA on hKIF4a DNA compaction, due to the 600 seconds of data in the absence of BSA and hKIF4a, shown in Fig. 4.8 B. The 600 seconds of data artificially inflates the value of the PDF, and yet the PDF value for the BSA and hKIF4a measurements is lower than the PDF value for the same measurements in the absence of BSA.

Chapter 5

Conclusion

To summarize this dissertation, I conducted an extensive survey of the literature about the effects of macromolecular crowding on DNA structure and identified three specific areas where research is lacking and provided motivation for investigation on those gaps. This is motivated by the fact that the cellular environment is highly crowded, while many laboratory measurements are conducted in dilute buffer, so introducing macromolecular crowders to laboratory settings is one step towards bridging the gap between *in vivo* and *in vitro* measurements. The first area in the literature that requires further research is using physiologically relevant crowders such as RNA or proteins, as opposed to synthetic polymers as crowders such as PEG or dextran. The second gap in the literature I identified was that most measurements investigating macromolecular crowders only use one size crowder at a time while the cellular environment contains crowding agents of varying sizes; this motivates further experiments with multiple sized crowders simultaneously. The final gap in the literature identified involves the connection between liquid-liquid phase separation (LLPS), the cellular environment, and macromolecular crowding. LLPS is critical to the formation of droplets and membraneless organelles within the highly crowded cell, additionally, macromolecular crowding has been shown to facilitate LLPS, yet the connection be-

tween macromolecular crowding and LLPS with biologically relevant materials has never been empirically proven.

The next chapter of this dissertation focused on my experimental works involving tethered particle motion measurements on the effects of macromolecular crowding on protein-mediated looping of DNA. In tethered particle motion experiments, a DNA tether is anchored to a substrate on one end and a protein-coated bead on the other end, this bead is subject to Brownian motion where it traverses a hemisphere with a radius dictated by the tether length. The 2D projection of the bead's location is recorded as a function of time as the bead traverses the hemisphere. For protein-mediated looping, there are two possible loop conformations, parallel and anti-parallel, as well as the unlooped conformation. The two looped conformation and the unlooped conformation are distinguished by the effective tether length, which is determined through analysis of the recorded 2D projection of beads location as a function of time. I conducted tethered particle motion experiments to investigate the effects of various concentrations of dextran 70 and bovine serum albumin (BSA) on LacI-mediated looping of DNA. From these measurements it was observed that when subject to macromolecular crowding, DNA favors the parallel loop conformation over the anti-parallel loop conformation, while the probability of DNA remaining unlooped is unaffected by crowding.

The fourth chapter of this dissertation focuses on further tethered particle motion experiments investigating hKIF4a compaction of DNA. KIF4a is a chromokinesin that has been hypothesized to contribute to the organization of mitotic chromosomes and the formation of chromosomal scaffolding. Measurements were initially conducted with bare DNA as a control measurement, followed by measurements with a truncated version of the protein with the DNA binding domain removed, which was indistinguishable from the bare DNA case. Measurements were then conducted with using 10 nM and 50 nM wild-type hKIF4a in the presence of ATP and AMP-PNP through

which it was observed that hKIF4a compacts DNA more efficiently in the presence of ATP, when compared with AMP-PNP. Further measurements with higher concentrations of wild-type hKIF4a showed that 100 nM compacted every DNA tether recorded, while 250 nM hKIF4a most likely maximally compacted every tether into tight globules such that all beads adhered to the surface of the substrate. The next set of experiments involved a variation of hKIF4a with the ATPase deleted at both 20 nM and 200 nM concentrations in the presence of ATP. This variation of hKIF4a compacted DNA to a greater extent than the wild-type hKIF4a in the presence of AMP-PNP, but to a lesser extent than the wild-type hKIF4a in the presence of ATP. The final set of experiments investigated the effects of macromolecular crowding on hKIF4a compaction of DNA; measurements began with a control sample that contained 5% BSA (w/v) and no hKIF4a. Upon adding 50 nM hKIF4a to samples with 5% BSA significant levels of DNA compaction were observed.

Bibliography

[1] Wenxuan Xu. *Supercoiling and Protein-mediated loops in Bacterial Transcription*. PhD thesis, Emory University, 2022.

[2] SangYoon Chung, Eitan Lerner, Yan Jin, Soohong Kim, Yazan Alhadid, Logan Wilson Grimaud, Irina X Zhang, Charles M Knobler, William M Gelbart, and Shimon Weiss. The effect of macromolecular crowding on single-round transcription by escherichia coli rna polymerase. *Nucleic acids research*, 47(3):1440–1450, 2019.

[3] Olivia Stiehl, Kathrin Weidner-Hertrampf, and Matthias Weiss. Corrigendum: Kinetics of conformational fluctuations in dna hairpin-loops in crowded fluids (2013 new j. phys. 15 113010). *New Journal of Physics*, 18(9):099501, 2016.

[4] Xiuli Cao, Bingjie Zhang, and Nanrong Zhao. Crowding-activity coupling effect on conformational change of a semi-flexible polymer. *Polymers*, 11(6):1021, 2019.

[5] Kazuki Kohata and Daisuke Miyoshi. Rna phase separation–mediated direction of molecular trafficking under conditions of molecular crowding. *Biophysical Reviews*, 12(3):669–676, 2020.

[6] Warren M. Mardoum, Stephanie M. Gorczyca, Kathryn E. Regan, Tsai-Chin Wu, and Rae M. Robertson-Anderson. Crowding induces entropically-driven

changes to dna dynamics that depend on crowder structure and ionic conditions. *Frontiers in Physics*, 6, 2018.

[7] Shane Scott, Cynthia Shaheen, Brendon McGuinness, Kimberly Metera, Fedor Kouzine, David Levens, Craig J Benham, and Sabrina Leslie. Single-molecule visualization of the effects of ionic strength and crowding on structure-mediated interactions in supercoiled dna molecules. *Nucleic acids research*, 47(12):6360–6368, 2019.

[8] R John Ellis and Allen P Minton. Join the crowd. *Nature*, 425(6953):27–28, 2003.

[9] Shu-Ichi Nakano, Daisuke Miyoshi, and Naoki Sugimoto. Effects of molecular crowding on the structures, interactions, and functions of nucleic acids. *Chemical reviews*, 114 5:2733–58, 2014.

[10] Daisuke Miyoshi and Naoki Sugimoto. Molecular crowding effects on structure and stability of DNA. *Biochimie*, 90:1040–1051, 2008.

[11] Steven B Zimmerman and Stefan O Trach. Estimation of macromolecule concentrations and excluded volume effects for the cytoplasm of escherichia coli. *Journal of molecular biology*, 222(3):599–620, 1991.

[12] B Bohrmann, M Haider, and E Kellenberger. Concentration evaluation of chromatin in unstained resin-embedded sections by means of low-dose ratio-contrast imaging in stem. *Ultramicroscopy*, 49(1-4):235–251, 1993.

[13] Yongdae Shin and Clifford P Brangwynne. Liquid phase condensation in cell physiology and disease. *Science (New York, N.Y.)*, 357(6357), September 2017.

[14] Irina M Kuznetsova, Boris Y Zaslavsky, Leonid Breydo, Konstantin K Tur-

overov, and Vladimir N Uversky. Beyond the excluded volume effects: mechanistic complexity of the crowded milieu. *Molecules*, 20(1):1377–1409, 2015.

[15] Alexander M Berezhkovskii and Attila Szabo. Theory of crowding effects on bimolecular reaction rates. *The Journal of Physical Chemistry B*, 120(26):5998–6002, 2016.

[16] Raphaela B Liebherr, Albert Hutterer, Matthias J Mickert, Franziska C Vogl, Andrea Beutner, Alfred Lechner, Helmut Hummel, and Hans H Gorris. Three-in-one enzyme assay based on single molecule detection in femtoliter arrays. *Analytical and bioanalytical chemistry*, 407(24):7443–7452, 2015.

[17] Space Studies Board, National Research Council, et al. *Size limits of very small microorganisms: proceedings of a workshop*. National Academies Press, 1999.

[18] Laura E Baltierra-Jasso, Michael J Morten, Linda Laflör, Steven D. Quinn, and Steven W. Magennis. Crowding-induced hybridization of single dna hairpins. *Journal of the American Chemical Society*, 137(51):16020–16023, December 2015.

[19] Vladimir B Teif and Klemen Bohinc. Condensed dna: condensing the concepts. *Progress in biophysics and molecular biology*, 105(3):208—222, May 2011.

[20] Laura Finzi and Wilma K Olson. The emerging role of dna supercoiling as a dynamic player in genomic structure and function. *Biophysical reviews*, 8(1):1–3, 2016.

[21] M Cristofalo, CA Marrano, D Salerno, R Corti, V Cassina, A Mammola, M Gherardi, Bianca Sclavi, M Cosentino Lagomarsino, and F Mantegazza. Cooperative effects on the compaction of dna fragments by the nucleoid protein h-ns and the crowding agent peg probed by magnetic tweezers. *Biochimica et Biophysica Acta (BBA)-General Subjects*, 1864(12):129725, 2020.

[22] Charles J Dorman. H-ns: a universal regulator for a dynamic genome. *Nature Reviews Microbiology*, 2(5):391–400, 2004.

[23] Sacha Lucchini, Gary Rowley, Martin D Goldberg, Douglas Hurd, Marcus Harrison, and Jay C D Hinton. H-ns mediates the silencing of laterally acquired genes in bacteria. *PLoS pathogens*, 2(8):e81, 2006.

[24] Shane C Dillon and Charles J Dorman. Bacterial nucleoid-associated proteins, nucleoid structure and gene expression. *Nature Reviews Microbiology*, 8(3):185–195, 2010.

[25] Niels Laurens, Rosalie PC Driessen, Iddo Heller, Daan Vorselen, Maarten C Noom, Felix JH Hol, Malcolm F White, Remus T Dame, and Gijs JL Wuite. Alba shapes the archaeal genome using a delicate balance of bridging and stiffening the dna. *Nature communications*, 3(1):1–8, 2012.

[26] Rosalie PC Driessen, Szu-Ning Lin, Willem-Jan Waterreus, Alson LH van der Meulen, Ramon A van der Valk, Niels Laurens, Geri F Moolenaar, Navraj S Pannu, Gijs JL Wuite, Nora Goosen, et al. Diverse architectural properties of sso10a proteins: Evidence for a role in chromatin compaction and organization. *Scientific reports*, 6(1):1–11, 2016.

[27] Wen-Bo Fu, Xiao-Ling Wang, Xing-Hua Zhang, Shi-Yong Ran, Jie Yan, and Ming Li. Compaction dynamics of single (dna) molecules under tension. *J. Am. Chem. Soc.*, 128 47:15040–15041, 2006.

[28] Jonathan Widom and Robert Baldwin. Monomolecular condensation of *lambda*-DNA induced by cobalt hexammine. *Biopolymers*, 22:1595–1620, 1983.

[29] P. G. Arscott, C. Ma, J. R. Wenner, and V. A. Bloomfield. DNA condensation by cobalt hexaammine III in alcohol-water mixtures: dielectric constant and other solvent effects. *Biopolymers*, 36:345–364, 1995.

[30] Andrew D Miller. Cationic liposomes for gene therapy. *Angewandte Chemie International Edition*, 37(13-14):1768–1785, 1998.

[31] G Krishnamoorthy, G Duportail, and Y Mély. Fluorescence dynamics of DNA condensed by the molecular crowding agent poly(ethylene glycol). *Biochemistry*, 41:15277–15287, 2002.

[32] G Krishnamoorthy, Bernard Roques, Jean-Luc Darlix, and Yves Mély. Dna condensation by the nucleocapsid protein of hiv-1: a mechanism ensuring dna protection. *Nucleic acids research*, 31(18):5425–5432, 2003.

[33] Mamata H Kombrabail and G Krishnamoorthy. Fluorescence dynamics of dna condensed by the molecular crowding agent poly (ethylene glycol). *Journal of fluorescence*, 15(5):741–747, 2005.

[34] LS Lerman. A transition to a compact form of dna in polymer solutions. *Proceedings of the National Academy of Sciences*, 68(8):1886–1890, 1971.

[35] Boris Obermeier, Frederik Wurm, Christine Mangold, and Holger Frey. Multifunctional poly (ethylene glycol) s. *Angewandte Chemie International Edition*, 50(35):7988–7997, 2011.

[36] Jesse V Jokerst, Tatsiana Lobovkina, Richard N Zare, and Sanjiv S Gambhir. Nanoparticle pegylation for imaging and therapy. *Nanomedicine*, 6(4):715–728, 2011.

[37] Danilo D Lasic. *Liposomes in gene delivery*. CRC press, 1997.

[38] Victor A Bloomfield. Dna condensation. *Current Opinion in Structural Biology*, 6(3):334–341, 1996.

[39] Renko de Vries. Dna condensation in bacteria: Interplay between macromolecular crowding and nucleoid proteins. *Biochimie*, 92(12):1715–1721, 2010. Special section "DNA and Chromosomes: Physical and Biological Approaches".

[40] Heikki Ojala, Gabija Ziedaite, Anders E Wallin, Dennis H Bamford, and Edward Hæggström. Optical tweezers reveal force plateau and internal friction in peg-induced dna condensation. *European Biophysics Journal*, 43(2-3):71–79, 2014.

[41] Weilin Xu and Susan J Muller. Polymer-monovalent salt-induced dna compaction studied via single-molecule microfluidic trapping. *Lab on a Chip*, 12(3):647–651, 2012.

[42] Ken Hirano, Masatoshi Ichikawa, Tomomi Ishido, Mitsuru Ishikawa, Yoshinobu Baba, and Kenichi Yoshikawa. How environmental solution conditions determine the compaction velocity of single dna molecules. *Nucleic acids research*, 40(1):284–289, 2012.

[43] E Froehlich, JS Mandeville, D Arnold, L Kreplak, and HA Tajmir-Riahi. Peg and mpeg–anthracene induce dna condensation and particle formation. *The Journal of Physical Chemistry B*, 115(32):9873–9879, 2011.

[44] H Kawakita, T Uneyama, M Kojima, K Morishima, Y Masubuchi, and H Watanabe. Formation of globules and aggregates of dna chains in dna/polyethylene glycol/monovalent salt aqueous solutions. *The Journal of chemical physics*, 131(9):094901, 2009.

[45] Takuya Saito, Takafumi Iwaki, and Kenichi Yoshikawa. Dna compaction induced by neutral polymer is retarded more effectively by divalent anion than monovalent anion. *Chemical Physics Letters*, 465(1-3):40–44, 2008.

[46] Kenichi Yoshikawa, Yuko Yoshikawa, Yoshiyuki Koyama, and Toshio Kanbe. Highly effective compaction of long duplex dna induced by polyethylene glycol with pendant amino groups. *Journal of the American Chemical Society*, 119(28):6473–6477, 1997.

[47] José Ésio Bessa Ramos, Renko de Vries, and João Ruggiero Neto. Dna ψ-condensation and reentrant decondensation: effect of the peg degree of polymerization. *The Journal of Physical Chemistry B*, 109(49):23661–23665, 2005.

[48] VV Vasilevskaya, AR Khokhlov, Y Matsuzawa, and K Yoshikawa. Collapse of single dna molecule in poly (ethylene glycol) solutions. *The Journal of chemical physics*, 102(16):6595–6602, 1995.

[49] HL Frisch and S Fesciyan. Dna phase transitions: the ψ transition of single coils. *Journal of Polymer Science: Polymer Letters Edition*, 17(5):309–315, 1979.

[50] Tom Maniatis, John H Venable Jr, and Leonard S Lerman. The structure of ψ dna. *Journal of molecular biology*, 84(1):37–64, 1974.

[51] K Minagawa, Y Matsuzawa, K Yoshikawa, AR Khokhlov, and M Doi. Direct observation of the coil-globule transition in dna molecules. *Biopolymers: Original Research on Biomolecules*, 34(4):555–558, 1994.

[52] Juan Pelta, Françoise Livolant, and Jean-Louis Sikorav. Dna aggregation induced by polyamines and cobalthexamine (). *Journal of Biological Chemistry*, 271(10):5656–5662, 1996.

[53] David Keller and Carlos Bustamante. Theory of the interaction of light with large inhomogeneous molecular aggregates. ii. psi-type circular dichroism. *The Journal of chemical physics*, 84(6):2972–2980, 1986.

[54] Chao Cheng, Jun-Li Jia, and Shi-Yong Ran. Polyethylene glycol and divalent salt-induced dna reentrant condensation revealed by single molecule measurements. *Soft Matter*, 11:3927–3935, 2015.

[55] Arnold Stein, James P Whitlock, and Minou Bina. Acidic polypeptides can assemble both histones and chromatin in vitro at physiological ionic strength. *Proceedings of the National Academy of Sciences*, 76(10):5000–5004, 1979.

[56] Valentin V Rybenkov, Alexander V Vologodskii, and Nicholas R Cozzarelli. The effect of ionic conditions on dna helical repeat, effective diameter and free energy of supercoiling. *Nucleic acids research*, 25(7):1412–1418, 1997.

[57] Tamar Schlick, Bin Li, and Wilma K Olson. The influence of salt on the structure and energetics of supercoiled dna. *Biophysical journal*, 67(6):2146–2166, 1994.

[58] Shane Scott, Zhi Ming Xu, Fedor Kouzine, Daniel J Berard, Cynthia Shaheen, Barbara Gravel, Laura Saunders, Alexander Hofkirchner, Catherine Leroux, Jill Laurin, et al. Visualizing structure-mediated interactions in supercoiled dna molecules. *Nucleic acids research*, 46(9):4622–4631, 2018.

[59] A Halperin and EB Zhulina. On the deformation behaviour of collapsed polymers. *EPL (Europhysics Letters)*, 15(4):417, 1991.

[60] A Craig and EM Terentjev. Stretching globular polymers. i. single chains. *The Journal of chemical physics*, 122(19):194901, 2005.

[61] Alexey A Polotsky, Elizaveta E Smolyakova, and Tatiana M Birshtein. Theory of mechanical unfolding of homopolymer globule: all-or-none transition in force-clamp mode vs phase coexistence in position-clamp mode. *Macromolecules*, 44(20):8270–8283, 2011.

[62] International Union of Pure and Applied Chemistry. Iupac compendium of chemical terminology – the gold book, 2009.

[63] Suparna Khatun, Anurag Singh, Kumari Shikha, Agneyo Ganguly, and Amar Nath Gupta. Plasmid dna undergoes two compaction regimes under macromolecular crowding. *ACS Macro Letters*, 11:186–192, 2022.

[64] Amar Nath Gupta and Johan RC van der Maarel. Compaction of plasmid dna by macromolecular crowding. *Macromolecules*, 50(4):1666–1671, 2017.

[65] Ce Zhang, Pei Ge Shao, Jeroen A van Kan, and Johan RC van der Maarel. Macromolecular crowding induced elongation and compaction of single dna molecules confined in a nanochannel. *Proceedings of the National Academy of Sciences*, 106(39):16651–16656, 2009.

[66] Steven B Zimmerman and Allen P Minton. Macromolecular crowding: biochemical, biophysical, and physiological consequences. *Annual review of biophysics and biomolecular structure*, 22(1):27–65, 1993.

[67] Xiaoying Zhu, Siow Yee Ng, Amar Nath Gupta, Yuan Ping Feng, Bow Ho, Alain Lapp, Stefan U Egelhaaf, V Trevor Forsyth, Michael Haertlein, Martine Moulin, et al. Effect of crowding on the conformation of interwound dna strands from neutron scattering measurements and monte carlo simulations. *Physical Review E*, 81(6):061905, 2010.

[68] Cole D Chapman, Stephanie Gorczyca, and Rae M Robertson-Anderson. Crowding induces complex ergodic diffusion and dynamic elongation of large dna molecules. *Biophysical journal*, 108(5):1220–1228, 2015.

[69] Stephanie M Gorczyca, Cole D Chapman, and Rae M Robertson-Anderson. Universal scaling of crowding-induced dna mobility is coupled with topology-

dependent molecular compaction and elongation. *Soft Matter*, 11(39):7762–7768, 2015.

[70] Jeffrey K Aronson. *Meyler's side effects of drugs: the international encyclopedia of adverse drug reactions and interactions*. Elsevier, 2015.

[71] Alan P Farwell and Susan A Dubord-Tomasetti. Thyroid hormone regulates the expression of laminin in the developing rat cerebellum. *Endocrinology*, 140(9):4221–4227, 1999.

[72] Boqun Liu, Christoffer Åberg, Floris J van Eerden, Siewert J Marrink, Bert Poolman, and Arnold J Boersma. Design and properties of genetically encoded probes for sensing macromolecular crowding. *Biophysical journal*, 112(9):1929–1939, 2017.

[73] Marcin Tabaka, Tomasz Kalwarczyk, Jedrzej Szymanski, Sen Hou, and Robert Holyst. The effect of macromolecular crowding on mobility of biomolecules, association kinetics, and gene expression in living cells. *Frontiers in Physics*, 2:54, 2014.

[74] R John Ellis. Macromolecular crowding: obvious but underappreciated. *Trends in biochemical sciences*, 26(10):597–604, 2001.

[75] Irina M Kuznetsova, Konstantin K Turoverov, and Vladimir N Uversky. What macromolecular crowding can do to a protein. *International journal of molecular sciences*, 15(12):23090–23140, 2014.

[76] Allen P Minton. Macromolecular crowding. *Current Biology*, 16(8):R269–R271, 2006.

[77] Stephen J Hagen. Solvent viscosity and friction in protein folding dynamics. *Current Protein and Peptide Science*, 11(5):385–395, 2010.

[78] David De Sancho, Anshul Sirur, and Robert B Best. Molecular origins of internal friction effects on protein-folding rates. *Nature communications*, 5(1):1–10, 2014.

[79] Stephen Busby, Annie Kolb, Henri Buc, H Buc, and T Strick. Where it all begins: an overview of promoter recognition and open complex formation, 2009.

[80] Ri Losick. In vitro transcription. *Annual Review of Biochemistry*, 41(1):409–446, 1972.

[81] Manchuta Dangkulwanich, Toyotaka Ishibashi, Lacramioara Bintu, and Carlos Bustamante. Molecular mechanisms of transcription through single-molecule experiments. *Chemical reviews*, 114(6):3203–3223, 2014.

[82] Ekaterina Sokolova, Evan Spruijt, Maike MK Hansen, Emilien Dubuc, Joost Groen, Venkatachalam Chokkalingam, Aigars Piruska, Hans A Heus, and Wilhelm TS Huck. Enhanced transcription rates in membrane-free protocells formed by coacervation of cell lysate. *Proceedings of the National Academy of Sciences*, 110(29):11692–11697, 2013.

[83] Maike MK Hansen, Lenny HH Meijer, Evan Spruijt, Roel JM Maas, Marta Ventosa Rosquelles, Joost Groen, Hans A Heus, and Wilhelm TS Huck. Macromolecular crowding creates heterogeneous environments of gene expression in picolitre droplets. *Nature nanotechnology*, 11(2):191–197, 2016.

[84] Eitan Lerner, SangYoon Chung, Benjamin L Allen, Shuang Wang, Jookyung Lee, Shijia W Lu, Logan W Grimaud, Antonino Ingargiola, Xavier Michalet, Yazan Alhadid, et al. Backtracked and paused transcription initiation intermediate of escherichia coli rna polymerase. *Proceedings of the National Academy of Sciences*, 113(43):E6562–E6571, 2016.

[85] Rafi Rashid, Stella Min Ling Chee, Michael Raghunath, and Thorsten Wohland. Macromolecular crowding gives rise to microviscosity, anomalous diffusion and accelerated actin polymerization. *Physical Biology*, 12(3):034001, 2015.

[86] Sen Hou, Piotr Trochimczyk, Lili Sun, Agnieszka Wisniewska, Tomasz Kalwarczyk, Xuzhu Zhang, Beata Wielgus-Kutrowska, Agnieszka Bzowska, and Robert Holyst. How can macromolecular crowding inhibit biological reactions? the enhanced formation of dna nanoparticles. *Scientific reports*, 6(1):1–11, 2016.

[87] Tomasz Kalwarczyk, Natalia Ziebacz, Anna Bielejewska, Ewa Zaboklicka, Kaloian Koynov, Jedrzej Szymanski, Agnieszka Wilk, Adam Patkowski, Jacek Gapinski, Hans-Jürgen Butt, et al. Comparative analysis of viscosity of complex liquids and cytoplasm of mammalian cells at the nanoscale. *Nano letters*, 11(5):2157–2163, 2011.

[88] Hendrik Anthony Kramers. Brownian motion in a field of force and the diffusion model of chemical reactions. *Physica*, 7(4):284–304, 1940.

[89] Kevin W Plaxco and David Baker. Limited internal friction in the rate-limiting step of a two-state protein folding reaction. *Proceedings of the National Academy of Sciences*, 95(23):13591–13596, 1998.

[90] Gouri S Jas, William A Eaton, and James Hofrichter. Effect of viscosity on the kinetics of α-helix and β-hairpin formation. *The Journal of Physical Chemistry B*, 105(1):261–272, 2001.

[91] Suzette A Pabit, Heinrich Roder, and Stephen J Hagen. Internal friction controls the speed of protein folding from a compact configuration. *Biochemistry*, 43(39):12532–12538, 2004.

[92] Grégoire Bonnet, Oleg Krichevsky, and Albert Libchaber. Kinetics of conforma-

tional fluctuations in dna hairpin-loops. *Proceedings of the National Academy of Sciences*, 95(15):8602–8606, 1998.

[93] Mark Ian Wallace, Liming Ying, Shankar Balasubramanian, and David Klenerman. Fret fluctuation spectroscopy: exploring the conformational dynamics of a dna hairpin loop. *The Journal of Physical Chemistry B*, 104(48):11551–11555, 2000.

[94] Mark I Wallace, Liming Ying, Shankar Balasubramanian, and David Klenerman. Non-arrhenius kinetics for the loop closure of a dna hairpin. *Proceedings of the National Academy of Sciences*, 98(10):5584–5589, 2001.

[95] Dominique Ernst, Marcel Hellmann, Jürgen Köhler, and Matthias Weiss. Fractional brownian motion in crowded fluids. *Soft Matter*, 8(18):4886–4889, 2012.

[96] Monique PJ Dohmen, Ana M Pereira, J Martin K Timmer, Nieck E Benes, and Jos TF Keurentjes. Hydrodynamic radii of polyethylene glycols in different solvents determined from viscosity measurements. *Journal of Chemical & Engineering Data*, 53(1):63–65, 2008.

[97] Matthias Weiss, Markus Elsner, Fredrik Kartberg, and Tommy Nilsson. Anomalous subdiffusion is a measure for cytoplasmic crowding in living cells. *Biophysical journal*, 87(5):3518–3524, 2004.

[98] Harry Walter and Donald E Brooks. Phase separation in cytoplasm, due to macromolecular crowding, is the basis for microcompartmentation. *FEBS letters*, 361(2-3):135–139, 1995.

[99] Brunno R Levone, Silvia C Lenzken, Marco Antonaci, Andreas Maiser, Alexander Rapp, Francesca Conte, Stefan Reber, Jonas Mechtersheimer, Antonella E Ronchi, Oliver Mühlemann, et al. Fus-dependent liquid–liquid phase separation is important for dna repair initiation. *Journal of cell biology*, 220(5), 2021.

[100] Anisha Shakya, Seonyoung Park, Neha Rana, and John T King. Liquid-liquid phase separation of histone proteins in cells: role in chromatin organization. *Biophysical journal*, 118(3):753–764, 2020.

[101] Sohee Park, Ryan Barnes, Yanxian Lin, Byoung-jin Jeon, Saeed Najafi, Kris T Delaney, Glenn H Fredrickson, Joan-Emma Shea, Dong Soo Hwang, and Songi Han. Dehydration entropy drives liquid-liquid phase separation by molecular crowding. *Communications Chemistry*, 3(1):1–12, 2020.

[102] HL Booij and HG Bungenberg de Jong. Colloid systems. In *Biocolloids and their Interactions*, pages 8–14. Springer, 1956.

[103] Aleksandr Ivanovich Oparin et al. The origin of life on the earth. *The origin of life on the earth.*, 1957.

[104] Russell J Stewart, James C Weaver, Daniel E Morse, and J Herbert Waite. The tube cement of phragmatopoma californica: a solid foam. *Journal of experimental biology*, 207(26):4727–4734, 2004.

[105] Hua Zhao, Chengjun Sun, Russell J Stewart, and J Herbert Waite. Cement proteins of the tube-building polychaete phragmatopoma californica. *Journal of Biological Chemistry*, 280(52):42938–42944, 2005.

[106] Clifford P Brangwynne, Christian R Eckmann, David S Courson, Agata Rybarska, Carsten Hoege, Jöbin Gharakhani, Frank Jülicher, and Anthony A Hyman. Germline p granules are liquid droplets that localize by controlled dissolution/condensation. *Science*, 324(5935):1729–1732, 2009.

[107] Hendrik Gerard Bungenberg de Jong. Crystallisation-coacervation-flocculation. *Colloid science*, 2:232–258, 1949.

[108] Allyson M Marianelli, Brian M Miller, and Christine D Keating. Impact of macromolecular crowding on rna/spermine complex coacervation and oligonucleotide compartmentalization. *Soft Matter*, 14(3):368–378, 2018.

[109] Salman F Banani, Hyun O Lee, Anthony A Hyman, and Michael K Rosen. Biomolecular condensates: organizers of cellular biochemistry. *Nature reviews Molecular cell biology*, 18(5):285–298, 2017.

[110] Simon Alberti. The wisdom of crowds: regulating cell function through condensed states of living matter. *Journal of cell science*, 130(17):2789–2796, 2017.

[111] Archa H Fox, Yun Wah Lam, Anthony KL Leung, Carol E Lyon, Jens Andersen, Matthias Mann, and Angus I Lamond. Paraspeckles: a novel nuclear domain. *Current Biology*, 12(1):13–25, 2002.

[112] Angus I Lamond and Judith E Sleeman. Nuclear substructure and dynamics. *Current biology*, 13(21):R825–R828, 2003.

[113] Mario Cioce and Angus I Lamond. Cajal bodies: a long history of discovery. *Annu. Rev. Cell Dev. Biol.*, 21:105–131, 2005.

[114] Thoru Pederson. The nucleus introduced. *Cold Spring Harbor Perspectives in Biology*, 3(5):a000521, 2011.

[115] Paul Anderson, Nancy Kedersha, and Pavel Ivanov. Stress granules, p-bodies and cancer. *Biochimica et Biophysica Acta (BBA)-Gene Regulatory Mechanisms*, 1849(7):861–870, 2015.

[116] Salman F Banani, Allyson M Rice, William B Peeples, Yuan Lin, Saumya Jain, Roy Parker, and Michael K Rosen. Compositional control of phase-separated cellular bodies. *Cell*, 166(3):651–663, 2016.

[117] Yuichi Yoshimura, Yuxi Lin, Hisashi Yagi, Young-Ho Lee, Hiroki Kitayama, Kazumasa Sakurai, Masatomo So, Hirotsugu Ogi, Hironobu Naiki, and Yuji Goto. Distinguishing crystal-like amyloid fibrils and glass-like amorphous aggregates from their kinetics of formation. *Proceedings of the National Academy of Sciences*, 109(36):14446–14451, 2012.

[118] Shana Elbaum-Garfinkle, Younghoon Kim, Krzysztof Szczepaniak, Carlos Chih-Hsiung Chen, Christian R Eckmann, Sua Myong, and Clifford P Brangwynne. The disordered p granule protein laf-1 drives phase separation into droplets with tunable viscosity and dynamics. *Proceedings of the National Academy of Sciences*, 112(23):7189–7194, 2015.

[119] Benjamin S Schuster, Ellen H Reed, Ranganath Parthasarathy, Craig N Jahnke, Reese M Caldwell, Jessica G Bermudez, Holly Ramage, Matthew C Good, and Daniel A Hammer. Controllable protein phase separation and modular recruitment to form responsive membraneless organelles. *Nature communications*, 9(1):1–12, 2018.

[120] Shogo Koga, David S Williams, Adam W Perriman, and Stephen Mann. Peptide–nucleotide microdroplets as a step towards a membrane-free protocell model. *Nature chemistry*, 3(9):720–724, 2011.

[121] J Ross Buchan. mrnp granules: assembly, function, and connections with disease. *RNA biology*, 11(8):1019–1030, 2014.

[122] Danièle Hernandez-Verdun. Assembly and disassembly of the nucleolus during the cell cycle. *nucleus*, 2(3):189–194, 2011.

[123] Archa H Fox and Angus I Lamond. Paraspeckles. *Cold Spring Harbor perspectives in biology*, 2(7):a000687, 2010.

[124] Valérie Lallemand-Breitenbach et al. Pml nuclear bodies. *Cold Spring Harbor perspectives in biology*, 2(5):a000661, 2010.

[125] Rivka Goobes, Nava Kahana, Orit Cohen, and Abraham Minsky. Metabolic buffering exerted by macromolecular crowding on dna- dna interactions: Origin and physiological significance. *Biochemistry*, 42(8):2431–2440, 2003.

[126] Allen P Minton. The effect of volume occupancy upon the thermodynamic activity of proteins: some biochemical consequences. *Molecular and cellular biochemistry*, 55(2):119–140, 1983.

[127] Donald J Winzor and Peter R Wills. Thermodynamic nonideality of enzyme solutions supplemented with inert solutes: yeast hexokinase revisited. *Biophysical chemistry*, 57(1):103–110, 1995.

[128] Allen P Minton. [7] molecular crowding: analysis of effects of high concentrations of inert cosolutes on biochemical equilibria and rates in terms of volume exclusion. *Methods in enzymology*, 295:127–149, 1998.

[129] Thomas L Madden and Judith Herzfeld. Crowding-induced organization of cytoskeletal elements: I. spontaneous demixing of cytosolic proteins and model filaments to form filament bundles. *Biophysical journal*, 65(3):1147–1154, 1993.

[130] Donna Louie and Philip Serwer. Quantification of the effect of excluded volume on double-stranded dna. *Journal of molecular biology*, 242(4):547–558, 1994.

[131] Lizabeth D Murphy and Steven B Zimmerman. Condensation and cohesion of λ dna in cell extracts and other media: Implications for the structure and function of dna in prokaryotes. *Biophysical chemistry*, 57(1):71–92, 1995.

[132] Jennifer Poon, Michael Bailey, Donald J Winzor, Barrie E Davidson, and William H Sawyer. Effects of molecular crowding on the interaction between dna

and the escherichia coli regulatory protein tyrr. *Biophysical journal*, 73(6):3257–3264, 1997.

[133] Paul Woolley and Peter R Wills. Excluded-volume effect of inert macromolecules on the melting of nucleic acids. *Biophysical chemistry*, 22(1-2):89–94, 1985.

[134] CH Spink and JB Chaires. Selective stabilization of triplex dna by poly (ethylene glycols). *Journal of the American Chemical Society*, 117(51):12887–12888, 1995.

[135] Charles H Spink and Jonathan B Chaires. Effects of hydration, ion release, and excluded volume on the melting of triplex and duplex dna. *Biochemistry*, 38(1):496–508, 1999.

[136] Stephanie C Weber, Andrew J Spakowitz, and Julie A Theriot. Bacterial chromosomal loci move subdiffusively through a viscoelastic cytoplasm. *Physical review letters*, 104(23):238102, 2010.

[137] Avelino Javer, Zhicheng Long, Eileen Nugent, Marco Grisi, Kamin Siriwatwetchakul, Kevin D Dorfman, Pietro Cicuta, and Marco Cosentino Lagomarsino. Short-time movement of e. coli chromosomal loci depends on coordinate and subcellular localization. *Nature communications*, 4(1):1–8, 2013.

[138] Bradley R Parry, Ivan V Surovtsev, Matthew T Cabeen, Corey S O'Hern, Eric R Dufresne, and Christine Jacobs-Wagner. The bacterial cytoplasm has glass-like properties and is fluidized by metabolic activity. *Cell*, 156(1-2):183–194, 2014.

[139] KE Polovnikov, M Gherardi, M Cosentino-Lagomarsino, and MV Tamm. Fractal folding and medium viscoelasticity contribute jointly to chromosome dynamics. *Physical review letters*, 120(8):088101, 2018.

[140] Theo Odijk. Osmotic compaction of supercoiled dna into a bacterial nucleoid. *Biophysical chemistry*, 73(1-2):23–29, 1998.

[141] Steven B Zimmerman. Studies on the compaction of isolated nucleoids from escherichia coli. *Journal of structural biology*, 147(2):146–158, 2004.

[142] Steven B Zimmerman. Shape and compaction of escherichia coli nucleoids. *Journal of structural biology*, 156(2):255–261, 2006.

[143] Steven B Zimmerman. Cooperative transitions of isolated escherichia coli nucleoids: implications for the nucleoid as a cellular phase. *Journal of structural biology*, 153(2):160–175, 2006.

[144] Paul A Wiggins, Remus Th Dame, Maarten C Noom, and Gijs JL Wuite. Protein-mediated molecular bridging: a key mechanism in biopolymer organization. *Biophysical journal*, 97(7):1997–2003, 2009.

[145] Remus T Dame and Mariliis Tark-Dame. Bacterial chromatin: converging views at different scales. *Current opinion in cell biology*, 40:60–65, 2016.

[146] Vincenzo G Benza, Bruno Bassetti, Kevin D Dorfman, Vittore F Scolari, Krystyna Bromek, Pietro Cicuta, and Marco Cosentino Lagomarsino. Physical descriptions of the bacterial nucleoid at large scales, and their biological implications. *Reports on Progress in Physics*, 75(7):076602, 2012.

[147] Marco Gherardi, Vittore Scolari, Remus Thei Dame, and Marco Cosentino Lagomarsino. Chromosome structure and dynamics in bacteria: Theory and experiments. In *Modeling the 3D Conformation of Genomes*, pages 207–230. CRC Press, 2019.

[148] Remus Thei Dame and Gijs JL Wuite. On the role of h-ns in the organization

of bacterial chromatin: From bulk to single molecules and back.... *Biophysical journal*, 85(6):4146–4148, 2003.

[149] Sónia Cunha, Theo Odijk, Erhan Süleymanoglu, and Conrad L Woldringh. Isolation of the escherichia coli nucleoid. *Biochimie*, 83(2):149–154, 2001.

[150] James Pelletier, Ken Halvorsen, Bae-Yeun Ha, Raffaella Paparcone, Steven J Sandler, Conrad L Woldringh, Wesley P Wong, and Suckjoon Jun. Physical manipulation of the escherichia coli chromosome reveals its soft nature. *Proceedings of the National Academy of Sciences*, 109(40):E2649–E2656, 2012.

[151] Anna S Wegner, Svetlana Alexeeva, Theo Odijk, and Conrad L Woldringh. Characterization of escherichia coli nucleoids released by osmotic shock. *Journal of structural biology*, 178(3):260–269, 2012.

[152] Vivek V Thacker, Krystyna Bromek, Benoit Meijer, Jurij Kotar, Bianca Sclavi, Marco Cosentino Lagomarsino, Ulrich F Keyser, and Pietro Cicuta. Bacterial nucleoid structure probed by active drag and resistive pulse sensing. *Integrative Biology*, 6(2):184–191, 2014.

[153] David Pastré, Loïc Hamon, Alain Mechulam, Isabelle Sorel, Sonia Baconnais, Patrick A Curmi, Eric Le Cam, and Olivier Piétrement. Atomic force microscopy imaging of dna under macromolecular crowding conditions. *Biomacromolecules*, 8(12):3712–3717, 2007.

[154] Stefan T Arold, Paul G Leonard, Gary N Parkinson, and John E Ladbury. H-ns forms a superhelical protein scaffold for dna condensation. *Proceedings of the National Academy of Sciences*, 107(36):15728–15732, 2010.

[155] Ricksen S Winardhi, Jie Yan, and Linda J Kenney. H-ns regulates gene expression and compacts the nucleoid: insights from single-molecule experiments. *Biophysical journal*, 109(7):1321–1329, 2015.

[156] David C Grainger. Structure and function of bacterial h-ns protein. *Biochemical society transactions*, 44(6):1561–1569, 2016.

[157] Yunfeng Gao, Yong Hwee Foo, Ricksen S Winardhi, Qingnan Tang, Jie Yan, and Linda J Kenney. Charged residues in the h-ns linker drive dna binding and gene silencing in single cells. *Proceedings of the National Academy of Sciences*, 114(47):12560–12565, 2017.

[158] Yuki Yamanaka, Ricksen S Winardhi, Erika Yamauchi, So-ichiro Nishiyama, Yoshiyuki Sowa, Jie Yan, Ikuro Kawagishi, Akira Ishihama, and Kaneyoshi Yamamoto. Dimerization site 2 of the bacterial dna-binding protein h-ns is required for gene silencing and stiffened nucleoprotein filament formation. *Journal of Biological Chemistry*, 293(24):9496–9505, 2018.

[159] Benjamin Lang, Nicolas Blot, Emeline Bouffartigues, Malcolm Buckle, Marcel Geertz, Claudio O Gualerzi, Ramesh Mavathur, Georgi Muskhelishvili, Cynthia L Pon, Sylvie Rimsky, et al. High-affinity dna binding sites for h-ns provide a molecular basis for selective silencing within proteobacterial genomes. *Nucleic acids research*, 35(18):6330–6337, 2007.

[160] Christina Kahramanoglou, Aswin SN Seshasayee, Ana I Prieto, David Ibberson, Sabine Schmidt, Jurgen Zimmermann, Vladimir Benes, Gillian M Fraser, and Nicholas M Luscombe. Direct and indirect effects of h-ns and fis on global gene expression control in escherichia coli. *Nucleic acids research*, 39(6):2073–2091, 2011.

[161] William Wiley Navarre, Steffen Porwollik, Yipeng Wang, Michael McClelland, Henry Rosen, Stephen J Libby, and Ferric C Fang. Selective silencing of foreign dna with low gc content by the h-ns protein in salmonella. *Science*, 313(5784):236–238, 2006.

[162] Blair RG Gordon, Yifei Li, Atina Cote, Matthew T Weirauch, Pengfei Ding, Timothy R Hughes, William Wiley Navarre, Bin Xia, and Jun Liu. Structural basis for recognition of at-rich dna by unrelated xenogeneic silencing proteins. *Proceedings of the National Academy of Sciences*, 108(26):10690–10695, 2011.

[163] Szu-Ning Lin, Gijs JL Wuite, and Remus T Dame. Effect of different crowding agents on the architectural properties of the bacterial nucleoid-associated protein hu. *International journal of molecular sciences*, 21(24):9553, 2020.

[164] Josette Rouviere-Yaniv and Francois Gros. Characterization of a novel, low-molecular-weight dna-binding protein from escherichia coli. *Proceedings of the National Academy of Sciences*, 72(9):3428–3432, 1975.

[165] Peter Hristov, Ivan Mitkov, Daniela Sirakova, Ivan Mehandgiiski, and Georgi Radoslavov. Measurement of casein micelle size in raw dairy cattle milk by dynamic light scattering. *Milk Proteins–From Structure to Biological Properties and Health Aspects. Published: September 7th*, 2016.

[166] PF Fox and A Brodkorb. The casein micelle: Historical aspects, current concepts and significance. *International dairy journal*, 18(7):677–684, 2008.

[167] K Devanand and JC Selser. Asymptotic behavior and long-range interactions in aqueous solutions of poly (ethylene oxide). *Macromolecules*, 24(22):5943–5947, 1991.

[168] Wei Yang, Jae Young Lee, and Marcin Nowotny. Making and breaking nucleic acids: two-mg2+-ion catalysis and substrate specificity. *Molecular cell*, 22(1):5–13, 2006.

[169] Rebecca L Coppins, Kathleen B Hall, and Eduardo A Groisman. The intricate world of riboswitches. *Current opinion in microbiology*, 10(2):176–181, 2007.

[170] Claudia Sissi and Manlio Palumbo. Effects of magnesium and related divalent metal ions in topoisomerase structure and function. *Nucleic acids research*, 37(3):702–711, 2009.

[171] Ashwani Kumar Vashishtha, Jimin Wang, and William H Konigsberg. Different divalent cations alter the kinetics and fidelity of dna polymerases. *Journal of Biological Chemistry*, 291(40):20869–20875, 2016.

[172] Arnold J Bloom. Metal regulation of metabolism. *Current opinion in chemical biology*, 49:33–38, 2019.

[173] Kenichi Yoshikawa, Seiko Hirota, Naoko Makita, and Yuko Yoshikawa. Compaction of dna induced by like-charge protein: opposite salt-effect against the polymer-salt-induced condensation with neutral polymer. *The Journal of Physical Chemistry Letters*, 1(12):1763–1766, 2010.

[174] Liel Sapir and Daniel Harries. Macromolecular stabilization by excluded cosolutes: mean field theory of crowded solutions. *Journal of chemical theory and computation*, 11(7):3478–3490, 2015.

[175] Liel Sapir and Daniel Harries. Macromolecular compaction by mixed solutions: Bridging versus depletion attraction. *Current Opinion in Colloid & Interface Science*, 22:80–87, 2016.

[176] Liel Sapir and Daniel Harries. Is the depletion force entropic? molecular crowding beyond steric interactions. *Current opinion in colloid & interface science*, 20(1):3–10, 2015.

[177] Shahar Sukenik, Liel Sapir, and Daniel Harries. Balance of enthalpy and entropy in depletion forces. *Current opinion in colloid & interface science*, 18(6):495–501, 2013.

[178] Sho Asakura and Fumio Oosawa. On interaction between two bodies immersed in a solution of macromolecules. *The Journal of chemical physics*, 22(7):1255–1256, 1954.

[179] Sho Asakura and Fumio Oosawa. Interaction between particles suspended in solutions of macromolecules. *Journal of polymer science*, 33(126):183–192, 1958.

[180] Jaeoh Shin, Andrey G Cherstvy, and Ralf Metzler. Kinetics of polymer looping with macromolecular crowding: effects of volume fraction and crowder size. *Soft matter*, 11(3):472–488, 2015.

[181] Syed Moiz Ahmed and Peter Dröge. Chromatin architectural factors as safeguards against excessive supercoiling during dna replication. *International Journal of Molecular Sciences*, 21(12):4504, 2020.

[182] Coline Arnould and Gaëlle Legube. The secret life of chromosome loops upon dna double-strand break. *Journal of Molecular Biology*, 432(3):724–736, 2020.

[183] Edward J Banigan and Leonid A Mirny. Loop extrusion: theory meets single-molecule experiments. *Current Opinion in Cell Biology*, 64:124–138, 2020.

[184] Ángela Sedeño Cacciatore and Benjamin D Rowland. Loop formation by smc complexes: turning heads, bending elbows, and fixed anchors. *Current opinion in genetics & development*, 55:11–18, 2019.

[185] Lydia Gramzow, Markus S Ritz, and Günter Theißen. On the origin of mads-domain transcription factors. *Trends in Genetics*, 26(4):149–153, 2010.

[186] Anders S Hansen, Claudia Cattoglio, Xavier Darzacq, and Robert Tjian. Recent evidence that tads and chromatin loops are dynamic structures. *Nucleus*, 9(1):20–32, 2018.

[187] Hiroyuki Hosokawa and Ellen V Rothenberg. How transcription factors drive choice of the t cell fate. *Nature Reviews Immunology*, 21(3):162–176, 2021.

[188] Omar L Kantidze and Sergey V Razin. Weak interactions in higher-order chromatin organization. *Nucleic Acids Research*, 48(9):4614–4626, 2020.

[189] Thøger Jensen Krogh, Andre Franke, Jakob Møller-Jensen, and Christoph Kaleta. Elucidating the influence of chromosomal architecture on transcriptional regulation in prokaryotes–observing strong local effects of nucleoid structure on gene regulation. *Frontiers in Microbiology*, page 2002, 2020.

[190] Michal Lazniewski, Wayne K Dawson, Anna Maria Rusek, and Dariusz Plewczynski. One protein to rule them all: The role of ccctc-binding factor in shaping human genome in health and disease. In *Seminars in cell & developmental biology*, volume 90, pages 114–127. Elsevier, 2019.

[191] David Umlauf and Raphaël Mourad. The 3d genome: From fundamental principles to disease and cancer. In *Seminars in Cell & Developmental Biology*, volume 90, pages 128–137. Elsevier, 2019.

[192] Szabolcs Semsey, Konstantin Virnik, and Sankar Adhya. A gamut of loops: meandering dna. *Trends in biochemical sciences*, 30(6):334–341, 2005.

[193] Virginia S Lioy, Axel Cournac, Martial Marbouty, Stéphane Duigou, Julien Mozziconacci, Olivier Espéli, Frédéric Boccard, and Romain Koszul. Multiscale structuring of the e. coli chromosome by nucleoid-associated and condensin proteins. *Cell*, 172(4):771–783, 2018.

[194] Jessica Zuin, Jesse R Dixon, Michael IJA van der Reijden, Zhen Ye, Petros Kolovos, Rutger WW Brouwer, Mariëtte PC van de Corput, Harmen JG van de Werken, Tobias A Knoch, Wilfred FJ van IJcken, et al. Cohesin and ctcf

differentially affect chromatin architecture and gene expression in human cells. *Proceedings of the National Academy of Sciences*, 111(3):996–1001, 2014.

[195] Wenxuan Xu, Yan Yan, Irina Artsimovitch, Nicolas Sunday, David Dunlap, and Laura Finzi. Transcription elongation through lac repressor-mediated dna loops. *bioRxiv*, 2021.

[196] Oi Kwan Wong, Martin Guthold, Dorothy A Erie, and Jeff Gelles. Interconvertible lac repressor–dna loops revealed by single-molecule experiments. *PLoS biology*, 6(9):e232, 2008.

[197] Baptiste Essevaz-Roulet, Ulrich Bockelmann, and Francois Heslot. Mechanical separation of the complementary strands of dna. *Proceedings of the National Academy of Sciences*, 94(22):11935–11940, 1997.

[198] M Wayne Davis and Erik M Jorgensen. Ape, a plasmid editor: a freely available dna manipulation and visualization program. *Frontiers in Bioinformatics*, page 5, 2022.

[199] Yan Yan, Yue Ding, Fenfei Leng, David Dunlap, and Laura Finzi. Protein-mediated loops in supercoiled dna create large topological domains. *Nucleic acids research*, 46(9):4417–4424, 2018.

[200] Sandip Kumar, Carlo Manzo, Chiara Zurla, Suleyman Ucuncuoglu, Laura Finzi, and David Dunlap. Enhanced tethered-particle motion analysis reveals viscous effects. *Biophysical journal*, 106(2):399–409, 2014.

[201] Lin Han, Bertrand H Lui, Seth Blumberg, John F Beausang, Philip C Nelson, and Rob Phillips. Calibration of tethered particle motion experiments. In *Mathematics of DNA structure, function and interactions*, pages 123–138. Springer, 2009.

[202] Daniel T Kovari, Yan Yan, Laura Finzi, and David Dunlap. Tethered particle motion: an easy technique for probing dna topology and interactions with transcription factors. In *Single Molecule Analysis*, pages 317–340. Springer, 2018.

[203] David G Priest, Sandip Kumar, Yan Yan, David D Dunlap, Ian B Dodd, and Keith E Shearwin. Quantitation of interactions between two dna loops demonstrates loop domain insulation in e. coli cells. *Proceedings of the National Academy of Sciences*, 111(42):E4449–E4457, 2014.

[204] Suleyman Ucuncuoglu, David A Schneider, Eric R Weeks, David Dunlap, and Laura Finzi. Multiplexed, tethered particle microscopy for studies of dna-enzyme dynamics. In *Methods in enzymology*, volume 582, pages 415–435. Elsevier, 2017.

[205] Yan Yan, Fenfei Leng, Laura Finzi, and David Dunlap. Protein-mediated looping of dna under tension requires supercoiling. *Nucleic acids research*, 46(5):2370–2379, 2018.

[206] Pasquale Strazzullo and Catherine Leclercq. Sodium. *Advances in Nutrition*, 5(2):188–190, 2014.

[207] Guikai Wu, Longen Zhou, Lily Khidr, Xuning Emily Guo, Wankee Kim, Young Mi Lee, Tatiana Krasieva, and Phang-Lang Chen. A novel role of the chromokinesin kif4a in dna damage response. *Cell Cycle*, 7(13):2013–2020, 2008.

[208] Cornelia Wandke, Marin Barisic, Reinhard Sigl, Veronika Rauch, Frank Wolf, Ana C Amaro, Chia H Tan, Antonio J Pereira, Ulrike Kutay, Helder Maiato, et al. Human chromokinesins promote chromosome congression and spindle microtubule dynamics during mitosis. *Journal of Cell Biology*, 198(5):847–863, 2012.

[209] Ana C Almeida and Helder Maiato. Chromokinesins. *Current Biology*, 28(19):R1131–R1135, 2018.

[210] Jeremy R Knowles. Enzyme-catalyzed phosphoryl transfer reactions. *Annual Review of Biochemistry*, 1980.

[211] Susanna Törnroth-Horsefield and Richard Neutze. Opening and closing the metabolite gate. *Proceedings of the National Academy of Sciences*, 105(50):19565–19566, 2008.

[212] Nobutaka Hirokawa. Kinesin and dynein superfamily proteins and the mechanism of organelle transport. *Science*, 279(5350):519–526, 1998.

[213] Rebecca Heald. Motor function in the mitotic spindle minireview. *Cell*, 102(4):399–402, 2000.

[214] Manjari Mazumdar and Tom Misteli. Chromokinesins: multitalented players in mitosis. *Trends in cell biology*, 15(7):349–355, 2005.

[215] J Richard McIntosh. Mitosis. *Cold Spring Harbor perspectives in biology*, 8(9):a023218, 2016.

[216] Elena Poser, Renaud Caous, Ulrike Gruneberg, and Francis A Barr. Aurora a promotes chromosome congression by activating the condensin-dependent pool of kif4a. *Journal of Cell Biology*, 219(2), 2020.

[217] Millipore Sigma. Amp-pnp adenylyl-imidodiphosphate amp-pnp.

[218] Harvey Lodish, Arnold Berk, Chris A Kaiser, Chris Kaiser, Monty Krieger, Matthew P Scott, Anthony Bretscher, Hidde Ploegh, Paul Matsudaira, et al. *Molecular cell biology*. Macmillan, 2008.